Design of Cryogenic Ejector Pump for Helium Liquefaction Plant to Produce Temperature Lower than 4 K

By

Shebaz Memon

12MMET13

DEPARTMENT OF MECHANICAL ENGINEERING
INSTITUTE OF TECHNOLOGY
NIRMA UNIVERSITY
AHMEDABAD-382481

May 2014

Design of Cryogenic Ejector Pump for Helium Liquefaction Plant to Produce Temperature Lower than 4 K

Major Project Report

Submitted in partial fulfillment of the requirements

For the Degree of

Master of Technology in Mechanical Engineering

(Thermal Engineering)

By

Shebaz Memon

(12MMET13)

Guided By

Dr. V J Lakhera

Mr. A. K. Sahu

DEPARTMENT OF MECHANICAL ENGINEERING
INSTITUTE OF TECHNOLOGY
NIRMA UNIVERSITY
AHMEDABAD-382481
May 2014

Declaration

This is to certify that

1. The thesis comprises of my original work towards the degree of Master of Technology in Mechanical Engineering (Thermal Engineering) at Nirma University and has not been submitted elsewhere for a degree.

2. Due acknowledgment has been made in the text to all other material used.

Shebaz Memon

12MMET13

Undertaking for Originality of the Work

I, Shebaz Memon, Roll. No. 12MMET13, give undertaking that the Major Project entitled "Design of Cryogenic Ejector Pump for Helium Liquefaction Plant to Produce Temperature Lower than 4 K" submitted by me, towards the partial fulfillment of the requirements for the degree of Master of Technology in Mechanical Engineering (Thermal) of Nirma University, Ahmedabad, is the original work carried out by me and I give assurance that no attempt of plagiarism has been made. I understand that in the event of any similarity found subsequently with any published work or any dissertation work elsewhere; it will result in severe disciplinary action.

Signature of Student

Endorsed by

(Signature of Guide)

Date: 14-05-2014
Place:Ahmedabad

Certificate

This is to certify that the Major Project Report entitled "**Design of Cryogenic Ejector Pump for Helium Plant to produce Temperature lower than 4 K**" submitted by **Mr Shebaz Memon(12MMET13)**, towards the partial fulfillment of the requirements for the award of Degree of Master of Technology in Mechanical Engineering (Thermal Engineering) of Institute of Technology, Nirma University, Ahmedabad is the record of work carried out by him under our supervision and guidance. In our opinion, the submitted work has reached a level required for being accepted for examination. The result embodied in this major project, to the best of our knowledge, has not been submitted to any other University or Institution for award of any degree.

Dr V J Lakhera,
Internal Guide and Professor,
Department of Mechanical Engineering,
Institute of Technology,
Nirma University,
Ahmedabad.

Mr A K Sahu,
External Guide and Scientist SF,
Divisional Head, Large Cryogenic
Plant and Cryo-system,
Institute for Plasma Research (IPR),
Bhat, Gandhinagar.

Dr R N Patel
Professor and Head,
Department of Mechanical Engineering,
Institute of Technology,
Nirma University,
Ahmedabad

Dr K Kotecha
Director,
Institute of Technology,
Nirma University,
Ahmedabad

Acknowledgments

It is my great pleasure to express thanks and profound gratitude to my university Guide, **Dr.V.J.Lakhera**, from Nirma University and external Guide **Mr.A.K.Sahu** from Institute for Plasma Research, Gandhinagar and also to **Dr. R.N Patel** HOD of Mechanical Engineering Department, Institute of Technology, Nirma University, Ahmedabad for their valuable guidance and continual encouragement throughout the semester. I am thankful to them for their valuable suggestion and conceptual clarity of the topic in detail that helped me a lot during this work.

I am very much thankful to **Dr. K. Kotecha** (Director, IT, NU) who have directly or indirectly helped me during this dissertation work.

I am also thankful to all faculty and staff members of Department of Mechanical Engineering, Nirma University, Ahmedabad for their special attention and suggestions for work.

The blessings of God and my family made the way for this dissertation work. I am very much grateful to them.

The friends, who always bear and motivated me throughout this training, I am thankful to them.

Shebaz Memon

Abstract

To produce temperature lower than 4 K in the proposed helium liquefaction (HeL) plant at Institute for Plasma Research(IPR), a pressure lower than atmospheric pressure in a Liquid Helium(LHe) chamber is to be produced by pumping helium vapor from the top of the chamber by the use of cryogenic ejector pump. The other method of creating subatmospheric pressure is by the use of cold compressor, which involves a rotating machine. Whereas the usage of a ejector pump does not involve any rotating parts and hence is a maintenance free equipment. The ejector pump is planned to be installed before the Joule-Thomson(J-T) valve of the helium Plant. The proposed design of HeL plant has two LHe chambers: the bigger one is to get LHe at the downstream of the J-T valve of the main process line whereas the smaller one is to get LHe through a branched process line just before the main J-T valve.The vapor from the smaller chamber is pumped to obtain a sub-atmospheric temperature over its liquid. This vapor is pumped by the ejector pump from below 1 bar to about 2 bar, which is then pushed to the main J-T valve for liquid Helium production at 4.5 K. The ejector pump is planned to produce refrigeration of about 300 W at 4 K. The design of ejector is usually done based on assumption of ideal gas behavior, whereas for the helium ejector working at less than 10 K, this assumption is not valid. A novel approach for the design of the ejector including real gas properties has been proposed, which uses the HEPAC software to obtain helium properties at that temperature range. This approach uses a fundamental approach to calculate the gain in kinetic energy(and thus by velocity of fluid) from enthalpy loss excluding the assumption of constant specific heat and adiabatic ratio required in standard gas dynamics approach. Computational Fluid Dynamics(CFD) simulation for the design obtained from real gas modeling approach is done using NIST REFPROP real gas database in ANSYS Fluent 14.5. The ejector design parameters like convergent angle of mixing chamber are not calculated from the analytical model. So the optimization of convergent angle, diffuser angle and constant area duct diameter is done using ANSYS Fluent 14.5. The present work explores the use of CFD as powerful tool to optimize the thermal design of ejector for low temperature applications.

Contents

List of Figures

List of Tables

Nomenclature

d	Diameter, m
r	Radius, m
A	Area, m^2
h	Enthalpy, Jkg^{-1}
$\dot{m}$	Mass flow rate, kgs^{-1}
a	Sonic Velocity, ms^{-1}
ρ	Density, kg/m^3
C_p	Specific heat of gas at constant pressure , $Jkg^{-1}K^{-1}$
C_v	Specific heat of gas at constant volume, $Jkg^{-1}K^{-1}$
P	Pressure, Pa
R	Gas constant, $Jkg^{-1}K^{-1}$
V	Gas velocity, ms^{-1}
T	Temperature, K
θ	Angle of convergent portion
γ	Heat ratio
x	Nozzle position, m
y	Position of hypothetical throat, m
η	Coefficient relating to the isentropic efficiency
ϕ	Coefficient of the loss of flow from section 1-1 to y-y
ω	Entrainment ratio

Superscripts

$*$	Critical mode of operation

Subscripts

c	Exit of ejector
co	Limiting condition of ejector operational mode
e	Inlet port of entrained flow
g	Nozzle inlet
m	Mixed flow
p	Primary flow
s	Suction or entrained flow
t	Nozzle throat
y	Location of chocking for the entrained flow
1	Nozzle exit

d	Diameter, m
2	Entrance of the constant-area section
3	Exit of the constant area section

Chapter 1

Introduction

1.1 Nuclear Fusion Reactor

1.1.1 Fusion Reactions

Fusion reaction is an atomic process by which cores of two light components wire to generate a quick, heavier core and a considerably quicker nucleon, i.e. a neutron or a proton. There is a little mass destruction, say m, between the beginning and the final reaction products which gets changed over into energy through Einstein's comparison $E = mc^2$, c being the velocity of light. This energy turns out as kinetic energy of the product particles and might be changed over into power by conventional techniques.

For such a reaction to happen, the responding cores need to have enough kinetic energy to conquer the repulsive electrostatic boundary between any two of them. For this to happen in lab explores, the responding particles need to be warmed to high temperatures, more than the temperature at the center of the sun. At such high temperatures, matter stays in plasma state, a gathering of charged particles.

A Deuterium and a Tritium core breaker to generate a Helium core and a neutron. The response transforms 17.6 MeV of vitality, out of which the Helium conveys 3.5 MeV and the neutron 14.1 MeV. In a plasma experiencing fusion, the reactions might act naturally managed, as a feature of the kinetic energy of the ensuing charged Helium could be utilized to keep up the precise high temperatures needed to maintain the combination reactions.

1.1.2 Importance of Fusion Energy

At the beginning of the 21st century, human society is faced with a precarious situation of increasing energy demands, especially from developing economies like India and China, coupled with a fast depleting conventional energy resources, which has been dominated by fossil fuel in the past century. The difference between the demand and the available supply has already started widening. This has led to and can potentially lead to in future conflicts of human societies, which can become a serious problem unless a viable extractable alternative energy resource(s) is not obtained quickly.

1.2 Liquid Helium Plant

Liquid Helium Plants (LHeP) are designed to produce liquid helium from any room temperature helium gas source with a minimum purity of 99%. The liquid helium (LHe) is produced and stored in the system's Dewar. A standard liquid helium plant as shown in Fig.1.1 consists of a cryorefrigerator with liquefaction heat exchangers, a liquid helium Dewar as well as a liquid helium level sensor and controller.

Room temperature helium gas enters the Dewar where it is liquefied and stored. A Pulse Tube Cryorefrigerator is used to liquefy the helium. The liquid helium plant is fully automatic and will shut down the cryorefrigerator when the Dewar is full. The liquid helium level controller indicates the liquid level in the Dewar and will automatically restart the system at a preset low level.

The operation of the Cryorefrigerator is based on a closed-loop helium expansion cycle. A complete system consists of two major components: one is the helium compressor package, which compresses refrigerant and removes heat from the system; the other is the cold head, which takes refrigerant through one or more additional expansion cycles to cool it down to cryogenic temperatures. The refrigerant gas used in the Cryorefrigerator is 99.999% pure helium. Flexible stainless steel lines called helium flex lines carry compressed helium from the compressor package to the cold head and carry low-pressure helium back.

The compressor package works as follows. An oil-lubricated compressor compresses the pure low-pressure helium that is returned from the cold head. The heat of compression is removed via a heat exchanger, and the oil from the compression process is removed in a series of oil separators and filters.

The compressed helium is then fed to the cold head via the high pressure helium flex line. In the cold head, adiabatic expansion of the helium and further heat removal allows cooling to cryogenic temperatures. The low-pressure helium then returns to the compressor package via the low-pressure helium flex line.

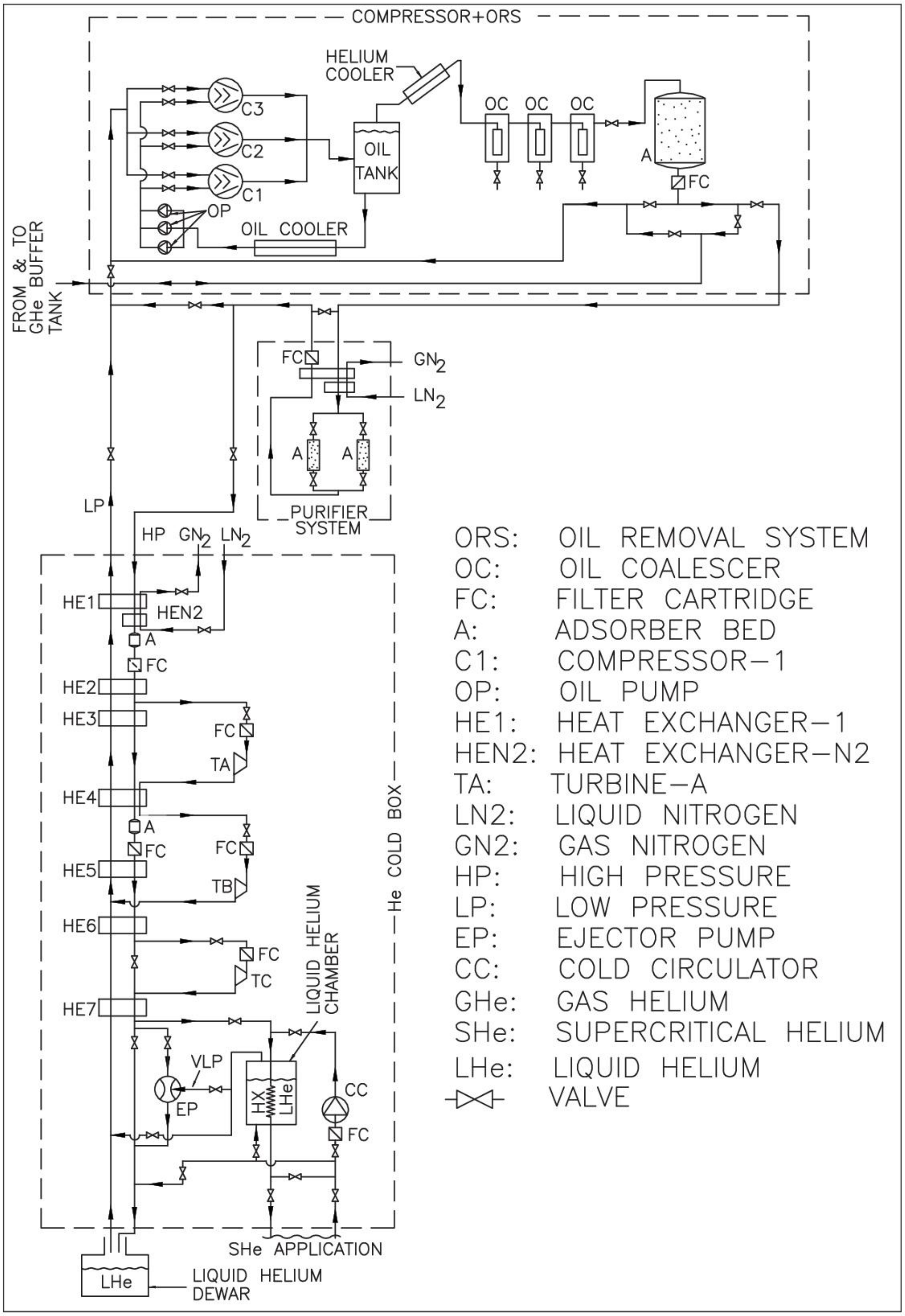

Figure 1.1: Helium liquefaction plant

Helium liquefier as the name suggest is used for the liquefaction process of Helium gas. In this plant there is compressor system in which three compressors are built up, after that there is a oil cooler in which oil needs to be cool down , then after as shown in Fig.1.1 there is a oil separator, in which the oil is removed from the mixture and after that helium cooler comes up, in which helium gets cooled down after that there are filters in which helium gas gets purified. After that cold box is there, the cold box shown below is used for the cool down and liquefaction purpose of Helium gas coming out of the Tokamak. The basic purpose of the two stream pre-cooling liquid nitrogen heat exchanger is to serve in the cooling down of the helium from 100K to 80K (normal operating conditions) and 310K to 80K (off-normal conditions).The liquid nitrogen used here remains at its saturation point leading to boiling conditions inside the heat exchanger, so that at the outlet of heat exchanger vapor nitrogen at 80K and He at 80K will be obtained. Hence, to fulfill its purpose liquid nitrogen uses its latent heat of vaporization and hence, making the process more efficient and fulfill its purpose to the fullest and also, avoiding the mixing of the streams at the outlet.

1.3 About Institute for Plasma Research(IPR)

Institute for Plasma Research - a premier research organization in India, is involved in research in various aspects of plasma science including basic plasma physics, magnetically confined hot plasmas and plasma technologies for industrial application. The institute is currently in the process of building a Steady State Superconducting Tokamak (SST-1) and is one of the partners in the International Thermonuclear Experimental Reactor(ITER) project.

The research areas can be broadly categorized into three activities:

• Studies on high temperature magnetically confined plasma

• Basic experiments in plasma physics including Free electron laser, dusty plasmas and other nonlinear phenomena

• Industrial plasma processing and application

• Current work on high temperature magnetically confined plasmas is being conducted in tokamak.

The plasma is formed by an electrical breakdown in an ultra high vacuum toroidal vessel and a current is inductively driven in the plasma. One has to use auxiliary heating schemes, since the efficiency to heat plasmas drops as the plasma temperature rises. Diagnostics like Thomson scattering for electron temperature measurement, soft X-ray camera and laser blow-off, are carried out on Aditya. A steady state tokamak the first of this kind in India, is being fabricated and set up, to study issues related to energy, particle and impurity confinement during steady state operation. Plasma disruptions and vertical displacement episodes will be studied. Non-inductive current drive would sustain the plasma current, and different aspects of the current drive would be studied.

The prototype fabrication of most of the components of the various subsystems of the tokamak has been completed, and is being tested, before final integration. Basic experiments, involving relatively cooler, rarer and less complicated plasmas are being carried out to understand the various facets of plasma that are difficult to study in bigger systems. Stability and equilibrium of toroidal plasma in the presence of radio frequency waves and new current drive mechanism with these waves is being studied. Issues related to excitation, propagation and linear, nonlinear interaction of whistler and helicon waves are being studied in a large volume plasma device. Free electron laser experiments and experiments to study dusty plasmas are also conducted

Equilibrium and non-equilibrium plasma properties can be exploited for commercial uses. A multi disciplinary team of physicists, engineers and material scientists are working together to generate advanced material processing technologies. Commercial prototype of medical waste pyrolisis system is some of the major activities concluded by the group at the Facilitation Centre for Industrial Plasma Technologies centre of IPR.

1.4 Motivation of Recent Study

Requirement of energy for the progress of mankind can be fulfilled by the fusion energy only if it can be achieved in a controlled environment. Initialization of the fusion reaction requires very high temperature and pressure condition as it is evident from Hydrogen bomb, where Deuterium mass requires the conventional fissile nuclear bomb around it to produce the pressure and temperature to start the fusion. A very important point here is that energy input to produce that high pressure and temperature condition should not be more than the extractable output of energy.

Production of very high temperature and pressure requires a very high electric current and superconductors to transmit it. These superconductors are to be maintained at very low temperature by liquid Helium. Cooling of superconductors through liquid helium involves evaporation, thus by phase change and large specific volume change, which makes it difficult to control the flow rate of helium. So super-critical helium is proposed to be used for certain cooling requirements, as shown in Fig.1.2. Supercritical helium is cooled in small Dewar by producing subatmospheric pressure above liquid bath to lower the evaporation point below 4 K. This subatmospheric pressure is to be produced by Ejector pump.

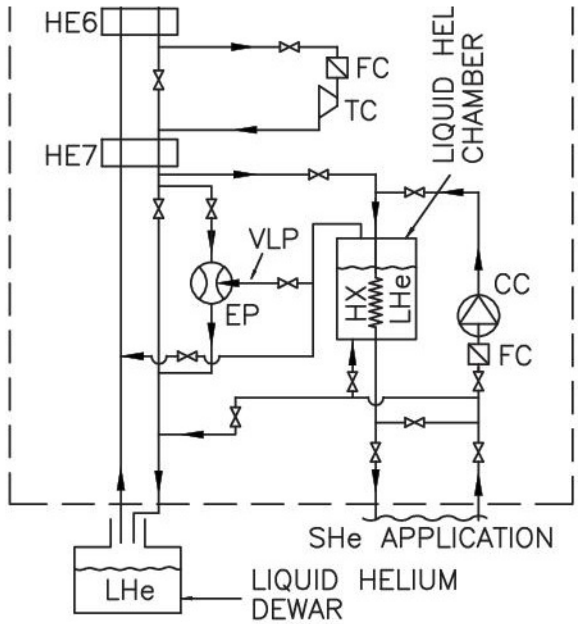

Figure 1.2: Magnified view of HeL plant

Rietdijk[4] first proposed the use of an ejector in cryogenic refrigerators. By using a cold ejector in place of a Joule-Thomson expansion valve in a closed-cycle helium refrigerator, subatmospheric pressure can be created in the volume over a liquid helium bath. The ejector pumps out the vapor from the bath, reducing the vapor pressure over the bath and thereby lowering the temperature of the bath. Since this is accomplished at cryogenic temperatures, low-pressure-drop (large-diameter) tubing and heat exchangers are not required to maintain the low pressures in the gas line between the bath and an external vacuum pump at ambient temperatures. Thus, a lower temperature can be obtained without necessitating the use of a vacuum pump or a room-temperature compressor at subatmospheric pressure. This eliminates air leakage, saves power, and permits the use of smaller heat exchangers within the system.

Other benefits of the ejector are that it is a simple, lightweight mechanical device that has no moving parts, does not require additional compressor power, and will not introduce any additional contaminants. The present study relates to study the design of a cryogenic ejector pump for the Helium Liquefaction plant to produce temperature lower than 4K.

Chapter 2

Literature Review

Detailed study of literature available on the subject of ejector was conducted and has been summarized as following.

2.1 Ejector Pump

In general, ejectors, exhausters or jet pumps, as they are called sometimes, are widely used in many industrial fields. Ejectors are employed in the power generation, chemical processing, nuclear industries, exhausting air from condensers, vacuum evaporation, distillation, and crystallization, refrigeration, drying, air conditioning, and for pumping large volumes of vapor and gas at low pressure. The main advantage of ejectors is that they have no pistons, valves, rotors, or any other moving parts, no lubrication or oil problems, nor extremely close tolerances and hence require little maintenance. They are, mechanically, the simplest of all of the present-day type of vacuum pumps.

Compared with mechanical pumps, ejectors have very low efficiencies when used in normal pumping applications but when a source of waste or low grade steam is available, a ejector may be cheaper to operate than a mechanical pump. Ejectors have many applications, such as heating, humidifying and pumping toxic and solids-bearing fluids, where a mechanical pump may be unsuitable.

2.2 Principle of Operation

A single stage steam ejector[1] depends for its pumping action on an expanding motive nozzle discharging a supersonic velocity jet at low pressure across a converging chamber as shown in Fig.2.1, which is connected to the equipment to be evacuated, and so bringing the suction fluid into intimate contact with the high-velocity motive fluid. The suction fluid is then entrained by the primary fluid and mixed with it in a parallel section. Then passing through a diffuser the velocity is reduced and discharge pressure recovered.

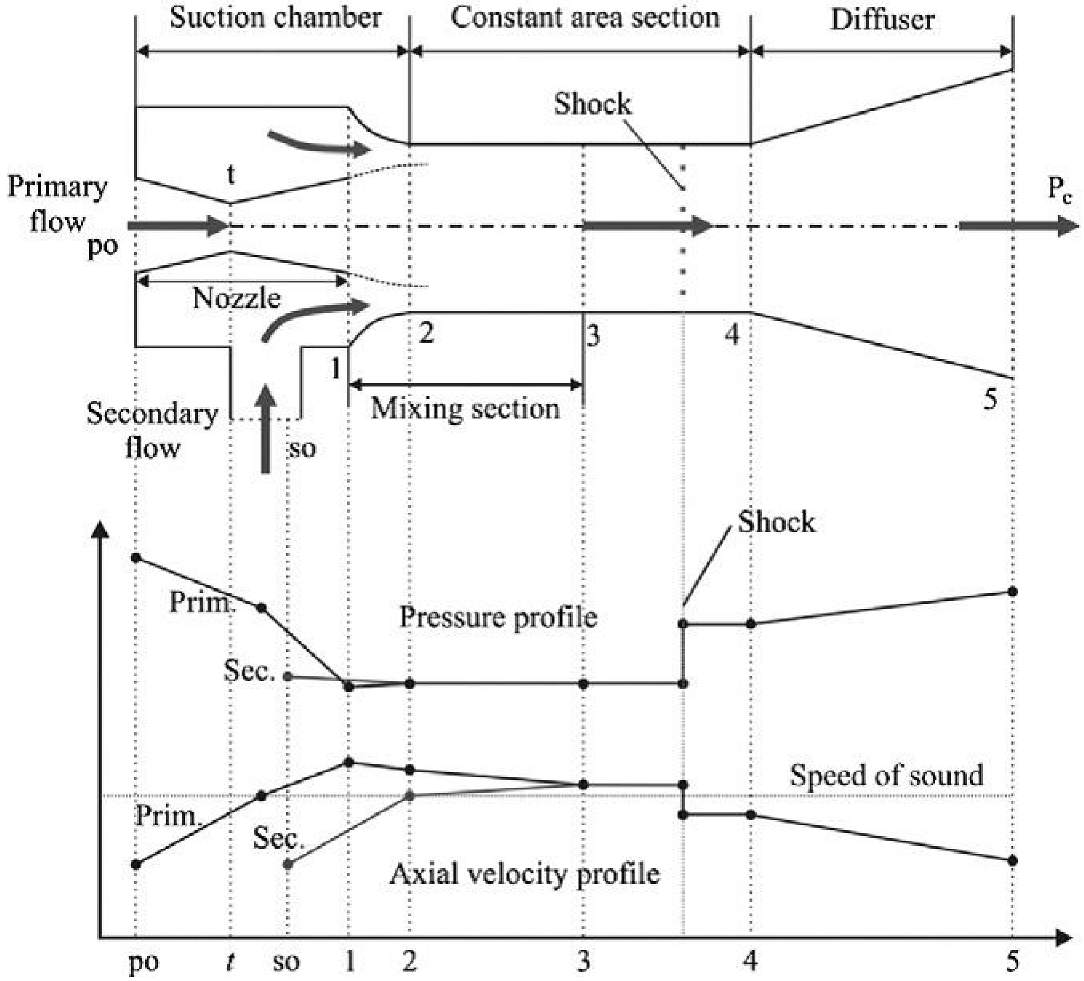

Figure 2.1: Ejector schematic diagram with pressure and velocity distribution [2]

Functionally, as mentioned earlier, a ejector is a device in which:

- The primary fluid, discharges from a high pressure region through a nozzle into a low pressure zone, developing a high velocity jet at low pressure for moving the fluid into the mixing chamber (i.e. the convergent section of the diffuser).
- The primary (or motive) fluid mixes with the secondary (entrained) fluid flow entering the mixing chamber (i.e. the parallel sections of the diffuser).
- The mixture flows through the divergent part of the diffuser to be discharged at a higher pressure than in the mixing chamber.

Considering the entrainment process it can be described by several stages that:

- Expansion of the jet to a pressure lower than of the entrained fluid flow pressure around the axis of the jet.
- Entrainment and diffusion action of the molecule of the entrained fluid by the viscous friction at the mating surface boundaries of the jet.
- Acceleration of the particles of the entrained fluid by impact with the particles from the primary fluid.

2.3 Historical Background

The study of jet action has[1], of late years, assumed greater importance owing to the large extent to which it is now employed in engineering process. The steam-jet ejector is a device known for a long time in the chemical industry under the name of "ejector". It is a pump which uses the action of steam to entrain the air.

From the experimental point of view, the subject appears to have been examined first by Napier in 1867, when passing steam at constant pressure through an orifice into a chamber maintained at some lower pressure. He found that the amount of steam passing through the orifice was a maximum when the pressure in the chamber was about half the value of the pressure at admission to the orifice. Any lowering of this back pressure produced no increase in the steam flow (Mellanby, 1928).

In 1886, Osborne Reynolds showed that in a nozzle of varying section the velocity at the minimum section could not exceed the velocity of sound in the fluid, hence, the lowest possible pressure at the exit of the orifice itself would be equal to that at which the pressure drop would produce a gas speed equal to the velocity of sound in the gas. The first successful application of the ejector as a vacuum producer was for surface condensers in the arrangement patented by Parsons, where the ejector worked in series with a reciprocating pump. In actual fact, steam ejectors find wide application in industry as a vacuum source because of their moderate investment, ease of operation, reasonable maintenance requirement and dependability.

Dependability is most essential, since an inoperative vacuum source can result in a severe yield penalty or even a plant shutdown. In spite of their wide application, until the late forties, usable design data were not available in the literature, and when an engineer had to design an ejector, most of the time, he resorted to trial and error, which may result in unsatisfactory performance or a waste of power, material, and labor.

Depending [5] on the position of the nozzle, there are two sorts of ejector outlines. At the point when the nozzle passageway is found inside the constant zone segment of the ejector, and the blending of primary and affected streams happens in the constant area section, the ejector is known as "constant area mixing ejector." The other, known as "constant pressure mixing ejector," is the point at which the nozzle passageway is spotted before the blending chamber, inside a convergent section before the constant region area. The current work concentrates on a constant-pressure blending ejector as a result of its enhanced execution over a constant zone blending ejector.

A few scientific models for ejectors have as of recently been created, typically focused around 1-D fluid dynamics hypothesis and expecting that the outspread speeds of both the primary and impelled streams are consistently distributed. First and foremost such numerical model was displayed by Keenan and Neumann (1942). Their model could anticipate the execution of a constant area blending ejector (without a diffuser), focused around perfect gas motion and the standards of preservation of mass, momentum, and energy. Later, Keenan et al. (1950) presented the idea of a constant pressure blending ejector, and expected that the pressures of the primary and affected streams are indistinguishable at the passageway of the primary nozzle, and that the blending of both streams begins at an uniform pressure up to the inlet of the constant zone segment without heat and friction losses.

2.4 Recent Work

Ejectors[4] have been used for many years near ambient temperature in refrigeration equipment, boilers, and chemical processing equipment. The principle of the ejector lies in the ability of a moving jet of primary fluid to entrain a secondary fluid and move it downstream. The ejector, then, is a simplified type of jet pump or compressor which pulls in the low pressure stream and increases the pressure of that stream by mixing it with the high pressure stream.

Huang et al.[6] (1999) assumed that the primary flow fans out without mixing with the induced flow after discharging from the exit of nozzle such that the mixing process starts beyond the hypothetical throat with a uniform pressure. Based on their assumption, built a model on the assumption that constant pressure mixing occurs inside the constant area section of the ejector to predict performance during critical operation.

WeiXiong Chen et al.[5] in their study proposed a 1-D model to predict the ejector performance not only at critical mode operation, but also at sub-critical mode operation. For validation purposes, the 1-D model results are compared to existing experimental data from the literature not only for the critical mode and also for the sub-critical mode, as well as data collected from a large-scale ejector facility.

A 1-D analysis for the prediction of ejector performance at critical-mode operation is carried out by Huang et al.[6] Constant-pressure mixing is assumed to occur inside the constant area section of the ejector and the entrained flow at choking condition is analyzed. They also carried out an experiment using 11 ejectors and R141b as the working fluid to verify the analytical results. The test results are used to determine the coefficients defined in the 1-D model by matching the test data with the analytical results. It is shown that the1-D analysis using the empirical coefficients can accurately predict the performance of the ejectors.

Cui Li et al. [7] described a numerical study of entrainment behavior and its configuration dependence for gas-gas and gas-liquid ejectors. A computational fluid dynamics (CFD) model is developed and experimental validation is undertaken over a wide range of operation conditions for ejector with different configurations. The predicted values by CFD simulation prove to be in good agreement with the experimental data. The investigation results indicate that pseudo-shock length has a dominant effect on entrainment performance and geometry optimization. Significant difference is noted in pseudo-shock length for gas-gas and gas liquid ejectors, and this is mainly because the viscosity similarity markedly differs within the range of 0.01-1.0, depending on the primary and secondary fluids of usage. Therefore the optimum mixing tube length to diameter ratio is about 1-2 for general gas-liquid ejectors while 5-7 for gas-gas ejectors. As an exception to the general gas-liquid ejectors, the optimum length to diameter ratio in He-LH_2 ejector is about 4, lying between that of the gas-gas ejector and gas-liquid ejector but still consistent with the pseudo-shock length. If the maximum allowable length of ejector mixing tube is less than the optimum value, placing the primary nozzle exit upstream of the mixing tube can greatly improve the entrainment performance.

Work by Yadav et al.[8] deals with optimization of the geometry of the suction chamber using computational fluid dynamics (CFD). The effect of (i) projection ratio i.e., ratio of the distance between the nozzle tip and throat to the throat diameter, (ii) the diameter of the suction chamber and (iii) the angle of the converging section on the entrainment rate of the secondary fluid have been studied. It was observed that for low values of projection ratio the entrainment rate was low. It increased with an increase in the projection ratio; however, became constant beyond a particular value of this ratio. The effect of the diameter of the suction chamber on the rate of entrainment was observed to be more complex. The entrainment rate showed a maximum value when the diameter of the suction chamber was varied over a wide range. The results obtained for different values of θ suggest that the optimum lies in the range of 5°-15°. The results have been explained on the basis of flow patterns produced.

The model by Hisham El-Dessouky et al.[9] gives the entrainment ratio as a function of the expansion ratio and the pressures of the entrained vapor, motive steam and compressed vapor. Also, correlations are developed for the motive steam pressure at the nozzle exit as a function of the evaporator and condenser pressures and the area ratios as a function of the entrainment ratio and the stream pressures. This allows for full design of the ejector, where defining the ejector load and the pressures of the motive steam, evaporator and condenser gives the entrainment ratio, the motive steam pressure at the nozzle outlet and the cross section areas of the diffuser and the nozzle. The developed correlations are based on large database that includes manufacturer design data and experimental data. The model includes correlations for the choked flow with compression ratios above 1.8. In addition, a correlation is provided for the non-choked flow with compression ratios below 1.8. The values of the coefficient of determination (R^2) are 0.85 and 0.78 for the choked and non-choked flow correlations, respectively. As for the correlations for the motive steam pressure at the nozzle outlet and the area ratios, all have R^2 values above 0.99.

In the study by Yinhai Zhu et al.[10] Computational Fluid Dynamics (CFD) technique is employed to investigate the effects of two important ejector geometry parameters: the primary Nozzle Exit Position (NXP) and the mixing section converging angle θ, on its performance. A CFD model is firstly established and calibrated by actual experimental data, and then used to create 95 different ejector geometries and tested under different working conditions. From 210 testing results, it is found that the optimum NXP is not only proportional to the mixing section throat diameter, but also increases as the primary flow pressure rises. On the other hand, the ejector performance is very sensitive to θ especially near the optimum working point. The entrainment ratio can vary as much as 26.6% by changing θ. A relatively bigger θ is required to better maximize the ejector performance when the primary flow pressure rises. The significance of the study is that these findings can be used to guide the adjustment of NXP and θ in order to obtain the best ejector system performance when the operating conditions are different from the on-design conditions.

Huang et al. [11] derived two empirical correlations from the test results of 15 ejectors for the performance prediction of ejectors using R141b as the working fluid. The ratio of the hypothetical throat area of the entrained flow to the nozzle throat area A_e/A_t, the geometric design parameter of the ejector A_3/A_t, and the pressure ratios P_g/P_t and P_c^*/P_e are used to correlate the performance of the ejector. The prediction of the entrainment ratio ω using the correlations is within ± 10% error. A method of calculation for the ejector design using the correlations is also developed. R141b is shown in the study to be a good working fluid for an ejector.

It was verified by T. Sriveerakul et al. [12] that the CFD method is an efficient tool to predict the entrainment ratio and critical back pressure of the ejector.The advantages of CFD over other conventional methods were proposed. Even though the errors of calculations were found to be quite large at some points, they could be clarified. However, it can be said that the CFD study in this research was just a pioneer study in the field of the ejector in refrigeration application. In order to utilize this method more efficiently, further studies are needed. From the study, it was shown that the constructed CFD model may not represent the experiment ejector perfectly; therefore, some improvements on the model setup and the calculation domain are needed. For instance, the real gas equations should be applied as the properties of the working fluid rather than using the perfect gas assumption. Moreover, the heat transfer function at the wall surfaces, that allows not only the investigation of heat transfer, but also of condensation during the process, should be turned on so that the model could be more realistic. In addition also shows another advantage of CFD over other analysis. Using the CFD, the graphic flow visualization of the modeled ejector could be created, and the phenomena inside the flow passage were explored.

In the paper by Yinhai Zhu et al. [13] a simple yet effective ejector model for a real time control and optimization of an ejector system is proposed. Firstly, a fundamental model for calculation of ejector entrainment ratio at critical working conditions is derived by one dimensional analysis and the shock circle model. Then, based on thermodynamic principles and the lumped parameter method, the fundamental ejector model is simplified to result in a hybrid ejector model. The model is very simple, which only requires two or three parameters and measurement of two variables to determine the ejector performance. Furthermore, the procedures for on line identification of the model parameters using linear and non-linear least squares methods are also presented. Compared with existing ejector models, the solution of the proposed model is much easier without coupled equations and iterative computations. Finally, the effectiveness of the proposed model is validated by published experimental data. Results show that the model is accurate and robust and gives a better match to the real performances of ejectors over the entire operating range than the existing models. This model is expected to have wide applications in real time control and optimization of ejector systems.

A friction based analytical formulation applicable to shock less diffusion in constant rate of momentum change (CRMC) ejector has been developed by Virendra Kumar [14] . The formulation predicts variation of different flow parameters viz., Mach number, static pressure, total pressure along the CRMC ejector. Further, numerical simulation and experimental study has been used to validate the analytical results. The analytical results are in reasonably good agreement with simulation and experimental results proving the efficacy of the model. Further, the benefit that accrues from using the present analytical model compared to isentropic model has also been presented. The static pressure prediction using present formulation shows a departure of 2.29% with respect to the numerical and 4% with experimental results, which is a marked improvement over a nearly 18% variation that occurs using isentropic formulation. Further, the utilized entrainment ratio for analytical computation is found to be within 3.45% relative error with numerical and 3% with experimental results at the design point exit pressure of 1.4 x 10^5 Pa. Hence, the present formulation may possibly enable better comprehension of CRMC based ejector performance with minimal increment in resources without the need for time intensive computational simulation.

Varga et al. studied [15] the numerical results for two 1 kW cooling capacity ejectors with variable primary nozzle geometry using R152a and R600a as working fluids. Working fluids were selected based on the criteria of low environmental impact and good performance in the range of operating conditions adequate for using solar thermal energy as primary heat source. Variable area ratio was achieved by applying a movable spindle at the primary nozzle inlet. Numerical results clearly show that adjusting spindle position resulted in a significant improvement of the entrainment ratio compared to a fixed geometry ejector when the operating conditions were different from design values. This increase in ejector performance was as high as 177% for low condenser pressures.

A jet-pump [16] design was developed by J. Fan et al. using an analytical approach and its efficiency was improved using an efficient and accurate computational fluid dynamics model of the compressible turbulent flow in the pump, whose predictions agreed well with corresponding experimental data. Parametric studies were performed to determine the influence of the pump's geometry on its performance and the high fidelity CFD solutions were used to build surrogate models of the pump's behavior using the moving least squares method. Global optimization was carried out using the surrogates. This approach resulted in pump efficiency increasing from 29% to 33% and enabled the energy requirements of the pump to be reduced by over 20%.

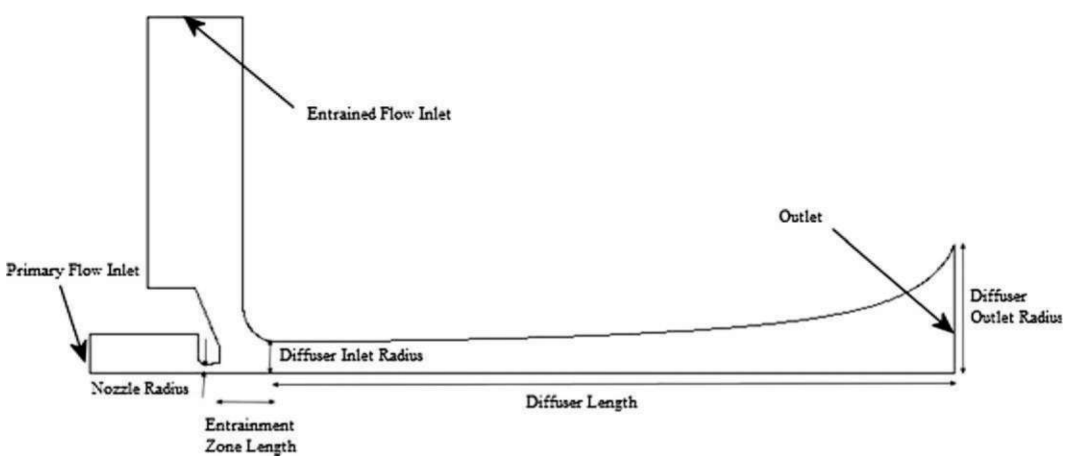

Figure 2.2: Axisymmetric model of ejector [16]

High fidelity CFD models of the compressible flow in jet pumps can be developed which agree well with experimental data, offering significant improvements over analytical methods.

The latter's inability to represent important flow physics, such as shock formation in the nozzle, preclude the use of a multi fidelity optimization strategy.

Appropriate combinations of solution algorithms and turbulence model provide the computational efficiency needed to embed CFD modeling within a formal optimization framework, using surrogate models and a genetic algorithm, which enable jet pump performance to be improved significantly. The CFD optimization study carried out here has enabled substantial improvements in jet-pump design to be achieved: pump efficiency has increased from 29% to 33% and, more significantly, the energy requirements of the pump have been reduced by over 20%.

The entrainment performance and the shock wave structures in a ejector were investigated numerically and experimentally by Yinhai Zhu et al. [17] Schlieren optical measurements were used to obtain pictures of the flow field structure in the ejector mixing chamber. A CFD model was used to obtain more detailed information about the flow, density and temperature distributions in the ejector. The main findings can be summarized as:

• The expansion waves in the shock train do not reach the mixing chamber wall when the ejector is working at the sub-critical mode. When the ejector is working in the critical mode, the shock is strong enough to separate the boundary layer and reflected shocks occur at the mixing chamber wall.

• The RNG k-ε model agrees best with experiments for predictions of both the mass flow rate and shock wave structures.

• The secondary flow mixes with the primary flow more fully and frequently for shock waves with shorter wavelengths. Thus, reducing the shock wave wavelength will improve the ejector performance.

A scientific model of the compressible transonic single and two-phase stream of a liquid is talked about by Jacek Smolka et al.[18]. The model was initially created recreate a refrigerant course through a heat pump ejector. In the proposed methodology, a temperature-based energy equation is supplanted with an enthalpy-based detailing, in which the specific enthalpy, rather than the temperature, is an autonomous variable. A thermodynamic and mechanical balance between vaporous and fluid phases is accepted for the two-phase stream. Thus, fluid properties, for example, the density, the dynamic viscosity and the diffusion coefficient, are characterized as capacities of the pressure and the specific enthalpy. The energy equation formulation is actualized in CFD programming utilizing subroutines that were created as a part of in-house. The plans was tried widely for a single phase stream of the R141b refrigerant, and for a two-phase stream of the R744 liquid (carbon dioxide) that happened in a model of the ejector motive nozzle. In the model acceptance method, a tasteful examination between the test and computational aftereffects of the primary and auxiliary mass stream rates was gotten for both stream administrations. What's more, on account of the R744 stream, the pressure appropriation along the focal point line of the ejector was precisely anticipated also. Besides, the results likewise demonstrates that geometry demonstrating and estimation correctness play an imperative in the last numerical results. As an aftereffect of the sensible computational times, this strategy could be successfully utilized for the configuration of ejectors and likewise in geometric advancement reckonings.

Different scientific models [19] have been proposed to evaluate the execution of ejector for distinctive operation and outline conditions. By and large, the numerical models are focused around the stream and blending phenomena inside the framework. They might be separated into two fundamental classifications as far as thermodynamic model and dynamic model. Inside the two classes, the models could be subdivided focused around streaming stages. Both thermodynamic model and dynamic model have two sorts: single-phase stream and two-phase stream. The single-phase stream thermodynamic model could be characterized into two sub-classes as indicated by the blending component: constant-pressure blending model and constant-area blending model. The two-stage element model might be further subdivided focused around the count systems: mixture model and Eulerian model. Likewise, utilizing the estimations information, a few exact/semi-observational models to assess the execution of ejector and to guide ejector outline has assessed.

Thermodynamic models are typically communicated in unequivocal logarithmic mathematical statements and are focused around the consistent state one dimensional model, concentrated on the pressure change brought on by supersonic shock. In these models, the nitty gritty nearby associations between shock waves and limit layers, their impact on blending and re-pressure rate are not considered. Lumped system is connected in the legislating mathematical statements which prompt basic model with easier exactness. To offer great exactness in anticipating the execution of the ejector by the thermodynamic model, some isentropic coefficients representing the friction loss were connected in the model and were controlled by examination. In these models, certain information on the chocking, shock and blending ought to be acquired ahead of time and suppositions ought to be made for model disentanglement. The more useful models known as constant-pressure blending model and constant-area blending model made the model doable. The constant pressure blending ejector gives preferred execution over the constant-area blending ejector. While the constant-area blending model gives more precise execution expectation. So as to give more faultless forecast, the two-stage streaming model is produced recognizing the buildup of the optional stream or the mixture of two streams in diverse stage states. In these models, quality is presented in the estimation of the state parameters. In spite of the fact that the overseeing mathematical statements are essentially the same as single-stage streaming model, the correctness is progressed.

The dynamic model, on the contrary, accounts the turbulence interaction between the primary and secondary stream, the shock reflection and chocking. It is more related to the actual process occurred in the ejector and the effect of the geometrical parameters and operation parameters can be well explained. The precision of this model is thus greatly improved.

2.5 Summary

Based on the literature survey, following points are noted:

- There are two sorts of ejector outlines. At the point when the nozzle passageway is found inside the constant area of the ejector, and the mixing of primary and entrained streams happens in the constant area segment, the ejector is known as "constant area mixing ejector." The other, known as "constant pressure mixing ejector," is the point at which the nozzle passageway is placed before the mixing chamber, inside an convergent section before the constant area. The current work concentrates on a constant-pressure mixing ejector in view of its enhanced execution over a constant area mixing ejector.

- Several numerical models for ejectors have as of recently been created, normally focused around 1-D fluid elements hypothesis and accepting that the outspread speeds of both the primary and entrained streams are consistently circulated.

- Due to the complex nature of the partial differential mathematical statements, it is important to tackle the numerical model utilizing numerical routines. Finite difference technique is perceived as the most correct and most all inclusive result procedure and is generally utilized in ejector displaying.

- The stream in the ejector is from supersonic to sonic, and afterward to subsonic. Accordingly, the decision of the turbulence model is vital. For compressible streaming model, it was discovered that RNG k-ε and k-ω-SST models were the best suited to anticipate the shock stage and the mean line of pressure recuperation. For incompressible stream the standard k-ε model and realizable k-ε model were widely used for time saving. For two-phase flowing model, the mixture model can give sensible results.

- It might be seen that the pressure inlet and pressure outlet limit conditions are generally utilized as a part of every last one of models at whatever point conceivable. Other limit conditions, for example, mass flow rate or velocity are occasional utilized as a part of models. For thermodynamic model, the assistant relations, for example, gas dynamic mathematical statements, the characterizing of Mach number and sonic speed, the state representation must be utilized to finish the scientific modelling.

- Besides, model approval is an essential work in model improvement since it offers the likelihood of contrasting reproduction results and genuine framework conduct. Tests are for the most part used to accept the numerical model. Other than, contrasting with the past numerical results is likewise a great acceptance technique.

Chapter 3

Analytical Design of Ejector

3.1 Introduction

The ejector [6] is classified into two types with respect to the position of the nozzle. The nozzle with its exit situated in the constant-area section of an ejector, the mixing of the primary and the entrained flow occurs inside the constant-area section and the ejector is known as "constant-area mixing ejector".For the nozzle with its exit situated within the suction chamber which is in front of the constant-area section, the ejector is known as "constant-pressure mixing ejector". For the constant pressure mixing ejector, as shown in Fig. 3.1, it is assumed that the mixing of the primary and the entrained streams takes place in the suction chamber with a uniform or constant pressure.

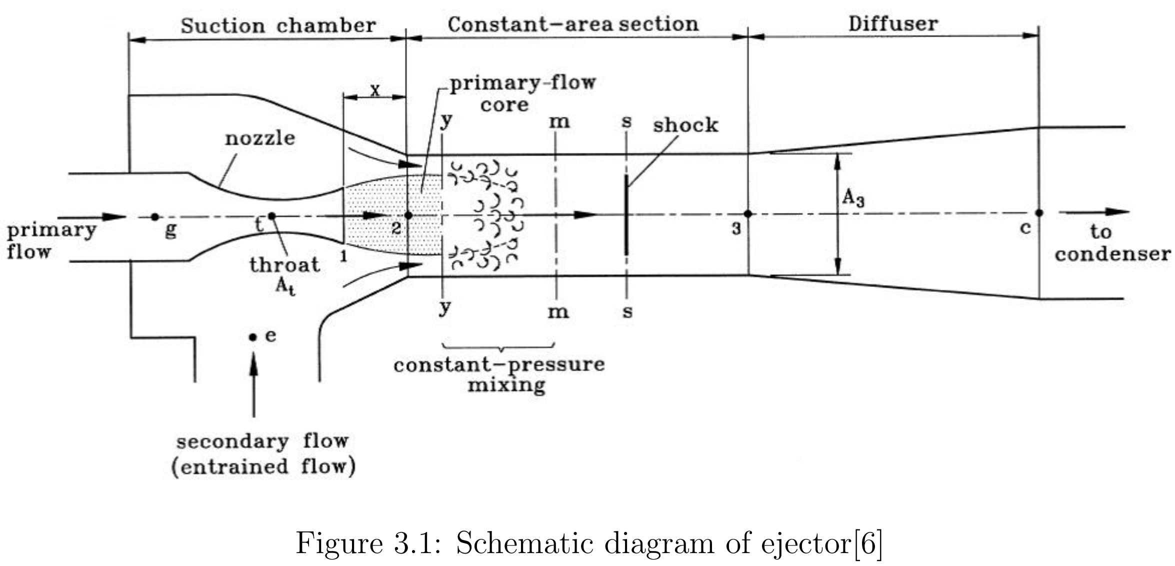

Figure 3.1: Schematic diagram of ejector[6]

It is known that the constant-pressure ejector gives better performance than the constant-area ejector and therefore widely used. The focus in this study is on the design of a "constant-pressure ejector".

The constant-pressure mixing theory of ejector is widely used in the analysis of constant-pressure ejector. Keenan et al. assumed that the pressures of the primary and the entrained flows at the exit of the nozzle have same pressure. Mixing of the primary and secondary fluid begins there with a uniform pressure, i.e. constant pressure, until the inlet of the constant-area section.

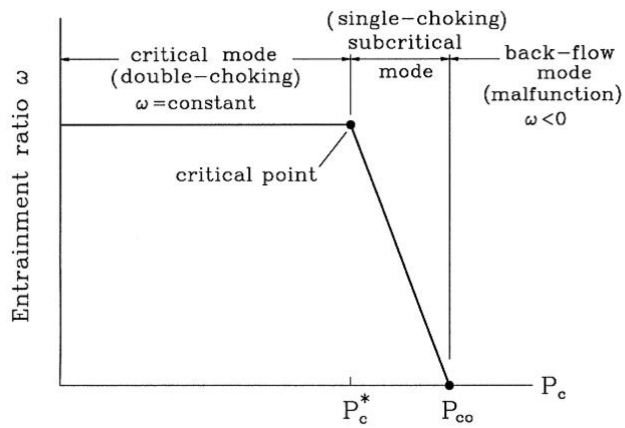

Figure 3.2: Operational modes of ejector[6]

If the ratio of the exit pressure ratio to the inlet pressure for the nozzle is such that chocking criteria is satisfied, the exit velocity from the nozzle will be supersonic. In this case Laval nozzle (convergent divergent nozzle) will be required.

In addition to the choking in the nozzle, the second choking of an ejector may take place due to the acceleration of the secondary flow from a stagnant state at secondary inlet to a sonic velocity flow in the mixing chamber at hypothetical throat.

Fig.3.2 shows the variation of entrainment ratio ω with the discharge or back pressure P_c for given secondary pressure P_e and fixed primary flow pressure P_g. The ejector performance can then be classified into three operational modes, according to the value of back pressure P_c

• double-choking or critical mode as $P_c < P_c^*$, when the primary and the secondary flows are both choking and the entrainment ratio is constant, i.e. ω constant;

• single-choking or subcritical mode as $P_c^* < P_c < P_{co}$, when only the primary flow is choked and secondary flow rate changes with the back pressure P_c; and

• back-flow or malfunction mode as $P_c{>}P_{co}$, when both the primary and the secondary flow are not choked and the entrained flow is reversed (malfunction), i.e.$\omega < 0$

3.2 Ejector Performance Analysis

The analytical design of the ejector mentioned in this section is based on Huang et al.[6].For the sack of analysis, it is assumed that the hypothetical throat occurs inside the constant-area section of the ejector. Thus, the mixing of two streams occurs inside the constant area section with a uniform pressure.

Assumptions made for the design of ejector are as following:

1. The working fluid is an ideal gas with constant specific heat C_p and adiabatic ratioγ.

2. The flow inside the ejector is steady and one dimensional.

3. For simplicity in derivation of the 1-D model, the isentropic relations are used as an approximation.For non-ideal process, the effects of frictional and mixing losses are taken into account by using some coefficients introduced in the isentropic relations. These coefficients are related to the isentropic efficiency and needs to be determined experimentally.

4. After exhausting from the nozzle, the primary flow fans out without mixing with the entrained flow until at some cross section y-y (hypothetical throat) which is inside the constant-area section.

5. The two streams starts to mix at the cross section y-y (hypothetical throat) with an uniform pressure, i.e. $P_{py} = P_{sy}$, before the shock which is at the cross section s-s.

6. The entrained flow is choked at the cross section y-y (hypothetical throat).

7. The inner wall of the ejector is adiabatic.

3.3 Governing Equations[6]

3.3.1 Primary flow through nozzle

For a given inlet stagnant pressure P_g and temperature T_g, the mass flow through the nozzle at choking condition follows the gas dynamic equation:

$$\dot{m}_p = \frac{P_g A_t}{\sqrt{T_g}} \times \sqrt{\frac{\gamma}{R}\left(\frac{2}{\gamma+1}\right)^{(\gamma+1)/(\gamma-1)}}\sqrt{\eta_p} \tag{3.1}$$

where η_p is a coefficient relating to the isentropic efficiency of the compressible flow in the nozzle. The gas dynamic relations between the Mach number at the exit of nozzle M_{p1} and the exit cross section area A_{p1} and pressure P_{p1} are, using isentropic relations as an approximation,

$$\left(\frac{A_{p1}}{A_t}\right)^2 \approx \frac{1}{M_{p1}^2}\left[\frac{2}{\gamma+1}\left(1+\frac{(\gamma-1)}{2}M_{p1}^2\right)\right]^{(\gamma+1)/(\gamma-1)} \tag{3.2}$$

$$\frac{P_g}{P_{p1}} \approx \left(1 + \frac{(\gamma-1)}{2} M_{p1}^2\right)^{\gamma/(\gamma-1)} \tag{3.3}$$

3.3.2 Primary-flow core (from exit of nozzle to hypothetical throat)

The Mach number M_{py} of the primary flow at the y-y section can be calculated from following equations an approximation:

$$\frac{P_{py}}{P_{p1}} \approx \frac{\left(1 + \frac{(\gamma-1)}{2} M_{p1}^2\right)^{\gamma/(\gamma-1)}}{\left(1 + \frac{(\gamma-1)}{2} M_{py}^2\right)^{\gamma/(\gamma-1)}} \tag{3.4}$$

The area of the primary flow core at the y-y section, the following isentropic relation is used, but an arbitrary coefficient ϕ_p is included to account for the loss of the primary flow from section 1-1 to y-y.

$$\frac{A_{py}}{A_{p1}} = \frac{(\phi_p/M_{py})\left[\frac{2}{\gamma+1}\left(1 + \frac{(\gamma-1)}{2} M_{py}^2\right)\right]^{(\gamma+1)/(\gamma-1)}}{(1/M_{p1})\left[\frac{2}{\gamma+1}\left(1 + \frac{(\gamma-1)}{2} \mathrm{M}_{\mathrm{p1}}^2\right)\right]^{(\gamma+1)/(\gamma-1)}} \tag{3.5}$$

The loss may result from the slipping or viscous effect of the primary and the entrained flows at the boundary. The loss actually reflects in the reduction of throat area Apy at y-y section through the introduction of the coefficient ϕ_p in Eq 5

3.3.3 Entrained flow from inlet to section y-y

From assumption (6), the entrained flow reaches choking condition at the y-y section, i.e. $M_{sy} = 1$. For a given inlet stagnant pressure, Pe

$$\frac{P_e}{P_{sy}} \approx \left(1 + \frac{(\gamma-1)}{2} M_{sy}^2\right)^{\gamma/(\gamma-1)} \tag{3.6}$$

The entrained flow rate at choking condition follows

$$\dot{m}_s = \frac{P_e A_{sy}}{\sqrt{T_e}} \times \sqrt{\frac{\gamma}{R}\left(\frac{2}{\gamma+1}\right)^{(\gamma+1)/(\gamma-1)}} \sqrt{\eta_p} \tag{3.7}$$

where η_s is the coefficient related to the isentropic efficiency of the entrained flow.

3.3.4 Cross-sectional area at section y-y

The geometrical cross-sectional area at section y-y is A_3 that is the sum of the areas for the primary flow A_{py} and for the entrained flow A_{sy}. That is,

$$A_{py} + A_{sy} = A_3 \tag{3.8}$$

3.3.5 Temperature and Mach number at section y–y

The temperature and the Mach number of the two stream at section y–y follows

$$\frac{T_g}{T_{py}} = 1 + \frac{(\gamma - 1)}{2} M_{py}^2 \tag{3.9}$$

$$\frac{T_e}{T_{sy}} = 1 + \frac{(\gamma - 1)}{2} M_{sy}^2 \tag{3.10}$$

3.3.6 Mixed flow at section m–m before the shock

Two streams starts to mix from section y-y. A shock then takes place with a sharp pressure rise at section s-s. A momentum balance relation thus can be derived as

$$\phi_m \left[\dot{m}_p V_{py} + \dot{m}_s V_{sy}\right] = \left(\dot{m}_p + \dot{m}_s\right) V_m \tag{3.11}$$

where V_m is the velocity of the mixed flow and ϕ_m is the coefficient accounting for the frictional loss [8]. Similarly, an energy balance relation can be derived as

$$\dot{m}_p \left(C_p T_{py} + \frac{V_{py}^2}{2}\right) + \dot{m}_s \left(C_p T_{sy} + \frac{V_{sy}^2}{2}\right) = \left(\dot{m}_p + \dot{m}_s\right) \left(C_p T_m + \frac{V_m^2}{2}\right) \tag{3.12}$$

where V_{py} and V_{sy} are the gas velocities of the primary and entrained flow at the section y-y

$a_{sy} = \sqrt{\gamma R T_{sy}}$

$$V_{py} = M_{py} \times a_{py} \tag{3.13}$$

$a_{sy} = \sqrt{\gamma R T_{sy}}$

$$V_{sy} = M_{sy} \times a_{sy} \tag{3.14}$$

The Mach number of the mixed flow can be evaluated using the following relation $M_m = \frac{V_m}{a_m}$

$$a_m = \sqrt{\gamma R T_m} \tag{3.15}$$

3.3.7 Mixed flow across the shock from section m–m to section 3–3

A supersonic shock will take place at section s-s with a sharp pressure rise. Assuming that the mixed flow after the shock undergoing an isentropic process, the mixed flow between section m-m and section 3-3 inside the constant area section has a uniform pressure P_3. Therefore, the following gas dynamic relations exist:

$$\frac{P_3}{P_m} = 1 + \frac{2\gamma}{\gamma+1}\left(M_m^2 - 1\right) \tag{3.16}$$

$$M_3^2 = \frac{1 + \left(\left(\gamma+1\right)/2\right) M_m^2}{\gamma M_m^2 - \left(\left(\gamma-1\right)/2\right)} \tag{3.17}$$

3.3.8 Mixed flow through diffuser

The pressure at the exit of the diffuser follows the relation, assuming isentropic process

$$\frac{P_c}{P_3} = \left(1 + \frac{(\gamma-1)}{2} M_3^2\right)^{\gamma/(\gamma-1)} \tag{3.18}$$

In the 1-D analysis, the coefficients accounting for the loss in the primary flow in the nozzle and in the suction flow before mixing are taken as $\eta_p = 0.95$ and $\eta_s = 0.85$, respectively. They are not very sensitive to the analytical results as the values adopted approximate that for isentropic process. The coefficient of the primary flow leaving the nozzle is taken as ϕ_p= 0.88. It was found that the loss coefficient in Eq.(11) is more sensitive than the other coefficients and should be taken to vary slightly with the ejector area ratio A_3/A_t in order to fit the test results. An empirical relation is found

$$\phi_m = \begin{cases} 0.80 & A_3/A_t > 8.3 \\ 0.82 & \leq A_3/A_t \leq 8.3 \\ 0.84 & A_3/A_t \leq 6.9 \end{cases} \tag{3.19}$$

3.4 Calculation of Flow Parameters and Geometric Parameters of Ejector

The flowchart of design simulation for 1-D ejector analysis is shown in Fig. 3.3.

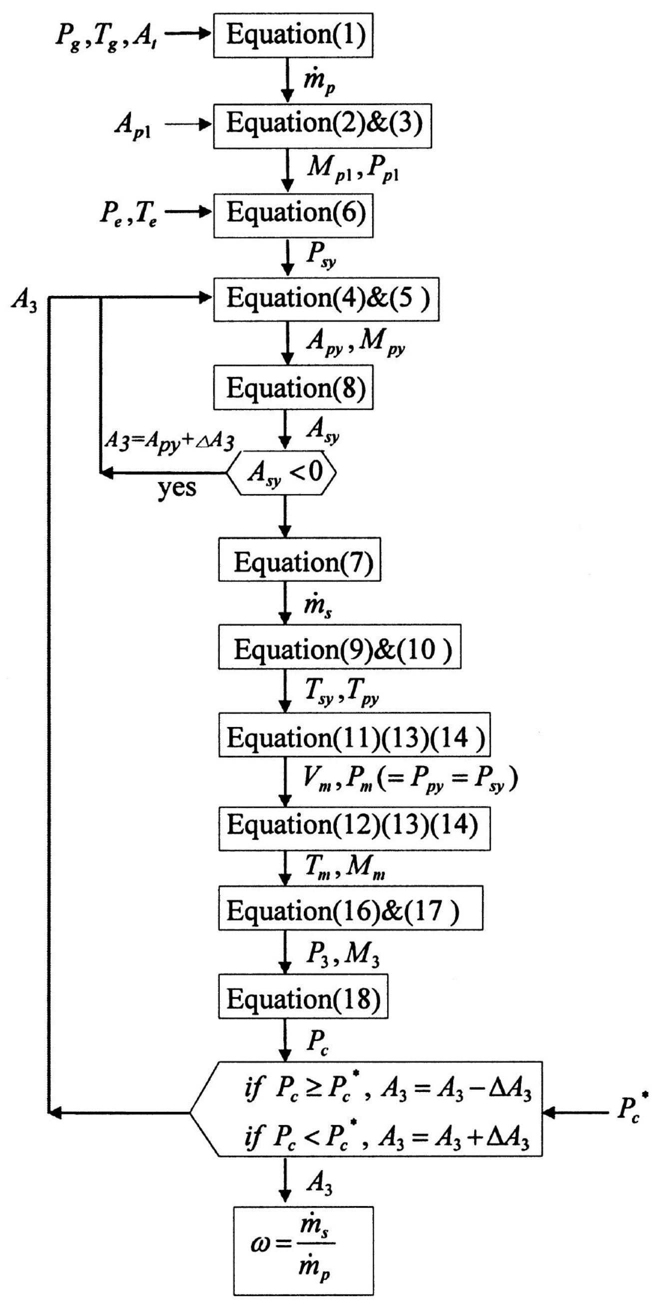

Figure 3.3: Simulation flowchart of the ejector performance analysis[6]

Inlet primary flow for the ejector is at 4 bar pressure and 10 K temperature with flow rate of 100g/s. Considering the heat ratio of Helium 1.9 in this temperature range and isentropic efficiency 0.95.

$$\dot{m}_p = \frac{P_g A_t}{\sqrt{T_g}} \times \sqrt{\frac{\gamma}{R}\left(\frac{2}{\gamma+1}\right)^{(\gamma+1)/(\gamma-1)}}\sqrt{\eta_p}$$

$$\Longrightarrow A_t = 17.90\ mm^2$$

$$\Longrightarrow d_t = 4.77mm$$

Mach No. at the exit of primary nozzle

$$\frac{P_g}{P_{p1}} \approx \left(1 + \frac{(\gamma-1)}{2} M_{p1}^2\right)^{\gamma/(\gamma-1)}$$

$$\Longrightarrow M_{p1} = 1.68$$

Exit of primary nozzle

$$\left(\frac{A_{p1}}{A_t}\right)^2 \approx \frac{1}{M_{p1}^2}\left[\frac{2}{\gamma+1}\left(1 + \frac{(\gamma-1)}{2} M_{p1}^2\right)\right]^{(\gamma+1)/(\gamma-1)}$$

$$\Longrightarrow A_{p1} = 22.03mm^2$$

$$\Longrightarrow d_{p1} = 5.298mm$$

Considering pressure drop of secondary flow through lining as 0.1 bar, entry entrained flow at 0.8 bar

$$\frac{P_e}{P_{sy}} \approx \left(1 + \frac{(\gamma-1)}{2} M_{sy}^2\right)^{\gamma/(\gamma-1)}$$

$$\Longrightarrow p_{sy} = 0.365bar$$

Mach no. of primary flow at chocking of entrained flow

$$\frac{P_{py}}{P_{p1}} \approx \frac{\left(1+\frac{(\gamma-1)}{2} M_{p1}^2\right)^{\gamma/(\gamma-1)}}{\left(1+\frac{(\gamma-1)}{2} M_{py}^2\right)^{\gamma/(\gamma-1)}}$$

$$\Longrightarrow M_{py} = 2.164$$

Area required for primary flow at y-y

$$\frac{A_{py}}{A_{p1}} = \frac{(\phi_p/M_{py})\left[\frac{2}{\gamma+1}\left(1 + \frac{(\gamma-1)}{2} M_{py}^2\right)\right]^{(\gamma+1)/(\gamma-1)}}{(1/M_{p1})\left[\frac{2}{\gamma+1}\left(1 + \frac{(\gamma-1)}{2} \mathrm{M}_{\mathrm{p1}}^2\right)\right]^{(\gamma+1)/(\gamma-1)}}$$

$$\Longrightarrow A_{py} = 24.86mm^2$$

Secondary entrained flow is 25 g/s at 4 K temperature and 0.8 bar pressure, so required area at y-y

$$\dot{m}_s = \frac{P_e A_{sy}}{\sqrt{T_e}} \times \sqrt{\frac{\gamma}{R}\left(\frac{2}{\gamma+1}\right)^{(\gamma+1)/(\gamma-1)}}\sqrt{\eta_p}$$

$\implies A_{sy} = 14.97mm^2$

Cross sectional area of mixing chamber

$A_{py} + A_{sy} = A_3$

$\implies A_3 = 39.83mm^2$

$\implies d_3 = 7.12mm$

Temperature of flow at y-y section

$\frac{T_g}{T_{py}} = 1 + \frac{(\gamma-1)}{2} M_{py}^2$

$\implies T_{py} = 3.22K$

$\frac{T_e}{T_{sy}} = 1 + \frac{(\gamma-1)}{2} M_{sy}^2$

$\implies T_{sy} = 2.76K$

velocity of flow at y-y section

$a_{py} = \sqrt{\gamma R T_{py}}$

$a_{py} = 41.88m/s$

$V_{py} = M_{py} \times a_{py}$

$V_{py} = 90.66m/s$

$a_{sy} = \sqrt{\gamma R T_{sy}}$

$a_{sy} = 38.97m/s$

$V_{sy} = M_{sy} \times a_{sy}$

$V_{sy} = 38.97m/s$

Velocity of mixed flow from momentum conservation considering flow loss ϕ_m

$\phi_m \left[\dot{m}_p V_{py} + \dot{m}_s V_{sy}\right] = (\dot{m}_p + \dot{m}_s) V_m$

$V_m = 70.68m/s$

Temperature of mixed flow from energy conservation

$\dot{m}_p \left(C_p T_{py} + \frac{V_{py}^2}{2}\right) + \dot{m}_s \left(C_p T_{sy} + \frac{V_{sy}^2}{2}\right) = (\dot{m}_p + \dot{m}_s) \left(C_p T_m + \frac{V_m^2}{2}\right)$

$T_m = 3.21K$

$M_m = \frac{V_m}{a_m} = 1.69$

$a_m = \sqrt{\gamma R T_m} = 41.84$

Pressure after normal shock

$\frac{P_3}{P_m} = 1 + \frac{2\gamma}{\gamma+1}\left(M_m^2 - 1\right)$

$\Longrightarrow P_3 = 1.235 bar$

Mach no. after normal shock

$M_3^2 = \frac{1+((\gamma+1)/2)M_m^2}{\gamma M_m^2-((\gamma-1)/2)}$

$\Longrightarrow M_3 = 0.67$

Pressure after diffusion

$\frac{P_c}{P_3} = \left(1 + \frac{(\gamma-1)}{2}M_3^2\right)^{\gamma/(\gamma-1)}$

$\Longrightarrow P_c = 1.85 bar$

3.5 Results and Discussion

Temperature and pressure of primary stream of Helium has been considered as variables for the calculations. Initially primary stream's total pressure has been varied from 12 bar to 2 bar for three different temperatures namely 300K, 150K and 10K. Efficiency of primary nozzle has been considered as 95%.

Exit pressure of primary nozzle has been decided to keep at 70kPa to suck the secondary flow at 80kPa. Ejector is designed as per double chocking conditions which means secondary flow reaches to sonic velocity before getting mixed with primary stream.

Coefficient for primary stream and coefficient of mixing length are 0.88 and 0.84 respectively. Calculation of flow parameters and geometric parameters has been done according to 1-D analysis. Mach no. at exit of primary nozzle is more than 1, which implies that Convergent-Divergent nozzle is required.

These calculation are for the primary flow inlet 100 gps and secondary flow of 25 gps.

Results of the same are tabulated in table3.1 .

It is evident from the Fig.3.4 that lower inlet pressure yields lower mach no. at the exit of primary nozzle, which results in smaller difference between throat diameter and exit diameter of primary nozzle. Therefore, radius of throat and radius of exit of nozzle are very similar at lower primary flow pressures.

For the given mass flow rate, increase in primary flow pressure gives smaller radius of nozzle and mixing chamber. For high pressure streams, smaller size of ejectors can be obtained.

P_g(Pa)	T_g(K)	T_{p1}(K)	M_{p1}	T_m(K)	r_t(mm)	r_{p1}(mm)	r_3(mm)	V_m(m/s)
1215900.00	300.00	77.60	2.52	122.62	5.30	7.34	12.44	1105.18
810600.00	300.00	94.03	2.21	129.71	6.49	8.24	13.05	1080.49
607950.00	300.00	107.76	1.99	135.64	7.49	8.98	13.56	1059.37
405300.00	300.00	130.57	1.70	145.53	9.17	10.20	14.43	1023.17
202650.00	300.00	181.32	1.21	167.64	12.97	13.14	16.47	936.89
1215900.00	150.00	38.80	2.52	55.43	4.45	6.18	9.52	755.80
810600.00	150.00	47.01	2.21	58.90	5.45	6.93	10.08	738.35
607950.00	150.00	53.88	1.99	61.81	6.30	7.55	10.55	723.41
405300.00	150.00	65.29	1.70	66.64	7.71	8.58	11.33	697.81
202650.00	150.00	90.66	1.21	77.44	10.91	11.05	17.83	636.80
1215900.00	10.00	2.59	2.52	3.77	2.26	3.14	4.95	196.67
810600.00	10.00	3.13	2.21	4.00	2.77	3.52	5.23	192.17
607950.00	10.00	3.59	1.99	4.19	3.20	3.84	5.46	188.31
405300.00	10.00	4.35	1.70	4.52	3.92	4.36	5.85	181.70
202650.00	10.00	6.04	1.21	5.24	5.54	5.61	10.98	165.95

Table 3.1: Effect of temperature of primary flow on geometry of ejector

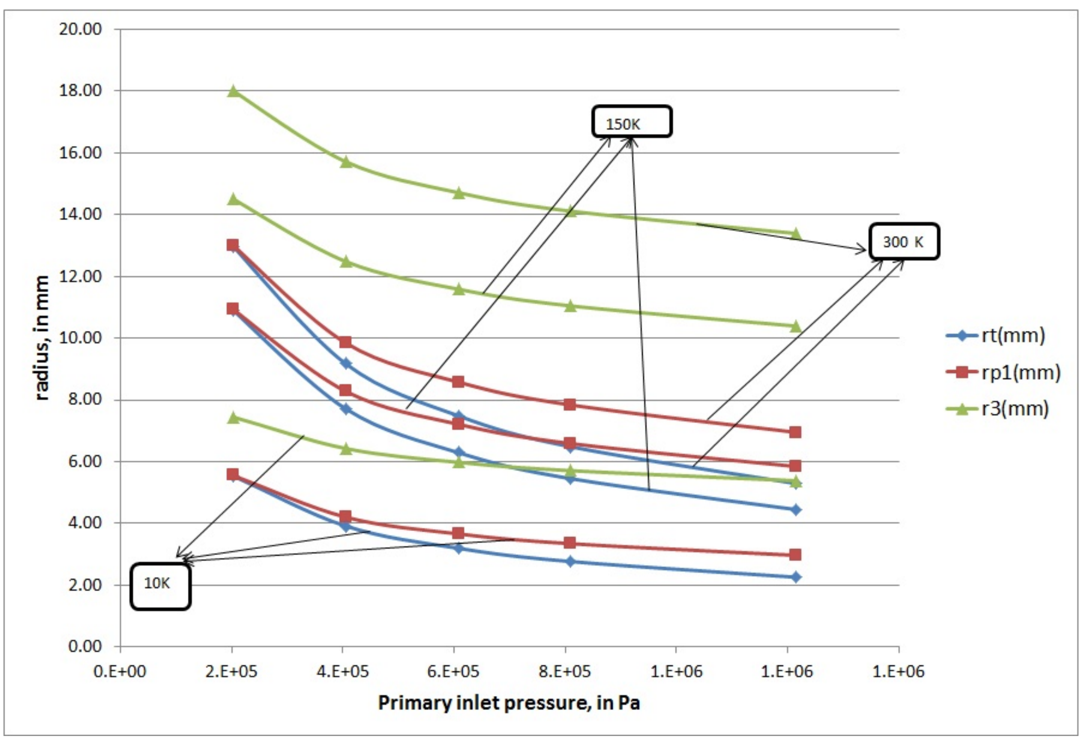

Figure 3.4: Primary nozzle throat radius, primary nozzle exit radius and mixing chamber radius for different pressure and temperatures of primary stream

Assumptions on which this model is constructed are not valid in the temperature range, where this ejector is required to function. The specific heat and adiabatic ratio of the fluid has been assumed to be constant. So It is needed to construct the model which takes into account the effects of varying fluid properties i.e. changing specific heat and adiabatic index of the Helium in cryogenic temperature range.

Chapter 4

A Novel Approach of Ejector Design for Real Gas Modeling

The design of ejector according to the methodology described in literature assumes that the gas behaves ideally and no variation in specific heat ratio is observed. Whereas in the case of helium ejector under consideration, the fluid has significant variation from ideal gas behavior in given working parameters range, so it requires a different approach for its design.

A novel approach for the design of the nozzle has been proposed, which uses real gas properties for calculation of the geometric parameters of the ejector. The primary stream nozzle has been divided in segments based on the pressure.

The inlet and outlet pressure of primary nozzle is 4bar and 80 kPa respectively and nozzle has been divided on pressure difference of 1000Pa. Model developed here is based on fundamental properties of fluid from HEPACK software. Stagnation enthalpy and stagnation entropy of inlet stream is also found from HEPACK. For every step, temperature, enthalpy, entropy and density are found through HEPAC for that decreased static pressure.

The difference between Stagnation enthalpy and static enthalpy gives the energy converted into kinetic energy, which in turn will give local velocity. And the sonic velocity at that point can be found from HEPAC, which will be useful to know the local Mach No.

As the velocity, density and mass flow rate are known, the cross-sectional area required for the flow of given mass flow rate is obtained as shown in 4.1.

Thus, this proposed model uses the properties of helium from HEPACK and avoids the use of any ideal gas relation, which eliminates the probability of misrepresentation of flow behavior. Input parameters for the design of the nozzle by real gas modelling are primary flow inlet pressure, temperature and exit pressure with flow rate required. The throat diameter and exit diameter of nozzle are obtained through this approach.

For the calculation of the mixing pressure at which the mixing will take place, secondary flow is segmented with difference of 1000Pa, too. The pressure at which the secondary flow reaches the sonic velocity will be considered to be mixing pressure.

The mixing pressure will be considered as reference pressure for the hypothetical throat, as until hypothetical throat the primary flow is assumed to be expanded. Primary flow dicretisation is extended up to this mixing pressure.

The application of mass conservation, momentum conservation and energy conservation equation are used to find the enthalpy and velocity of mixed flow. This mixed flow, if supersonic will create shock in constant area duct. Fluid after the shock is compressed in diffuser to recover the pressure at the discharge of the ejector.

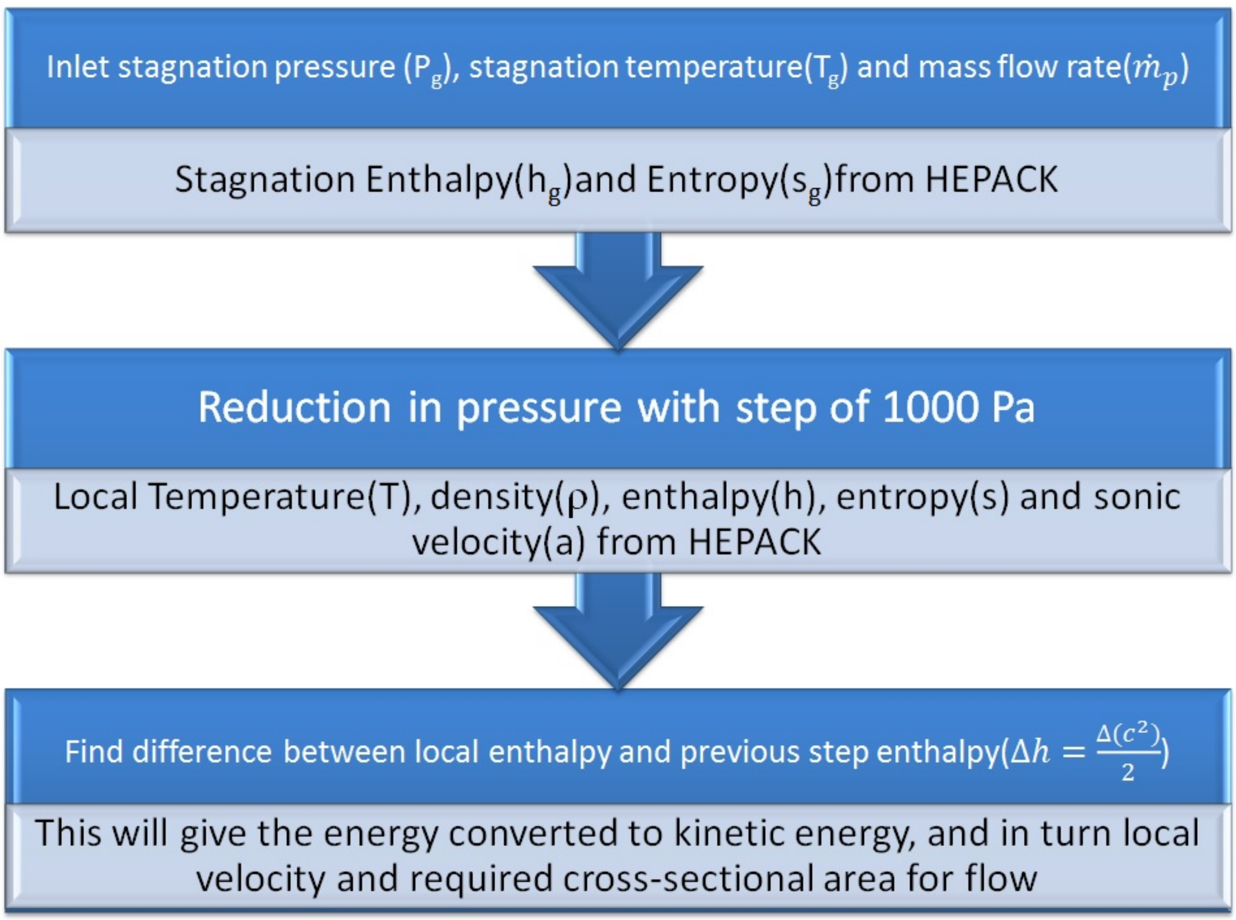

Figure 4.1: Process flow diagram for nozzle design

The mass flow rate, local density and local velocity give the required cross sectional area at given pressure for the flow to take place. The sample of detailed design procedure is shown in appendix-I.

4.1 Ejector Design for 300K Primary Flow Inlet

Ejector design by segmentation approach is applied for 300K primary inlet with different pressures, which gives geometrical parameters as described below.This design for ejector with inclusion of real gas properties has been for the varying primary inlet pressure from 14 bar to 1.5 bar for entrained pressure 80kPa. Results for the same are tabulated in Table 4.1.

Table 4.1: Ejector design for 300K primary inlet and mass flow rate of 100 gps

P_g(Pa)	r_t(mm)	r_{p1}(mm)	T_{p1}(K)	r_1(mm)	r_m(mm)	r_c(mm)	P_c(Pa)
1418550	4.94	7.59	90.07	14.16	9.06	18.17	599472.94
1215900	5.34	7.88	95.80	14.31	9.39	18.89	554678.46
810600	6.65	8.73	112.65	14.80	10.32	20.98	449064.16
607950	8.27	9.89	136.71	15.51	11.50	23.73	351007.07
405300	9.24	10.58	148.62	15.30	11.59	23.93	345072.52
303975	10.67	11.57	166.74	16.64	13.04	27.47	261848.69
202650	13.07	13.35	196.10	17.92	14.61	31.49	199179.27
151988	15.09	15.10	220.01	19.25	15.96	41.33	115619.82

The outlet of the nozzle has been kept at 70kPa for these calculation, which implies that lower Mach No. of the primary stream will be obtained at the exit of nozzle. This is evident from the Fig.4.2, where the difference between throat radius of the nozzle and radius of the exit of nozzle goes on increasing with rise in inlet pressure of the nozzle.

Figure 4.2: Nozzle throat radius, nozzle exit radius and convergent portion inlet radius for 300K primary stream inlet

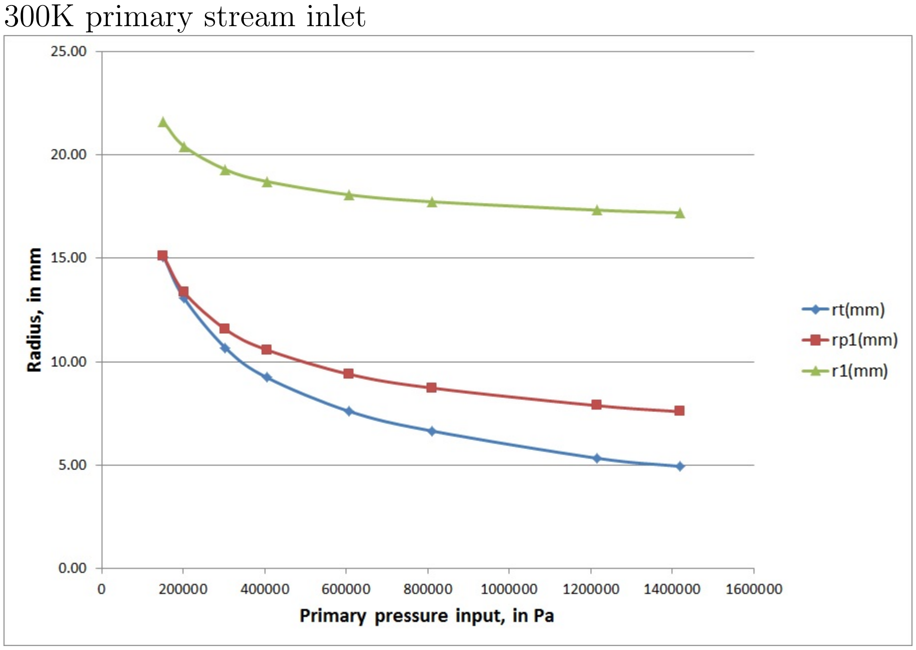

The lower pressure stream after blending will require larger cross-sectional area for the given mass flow rate as shown in Fig.4.3.

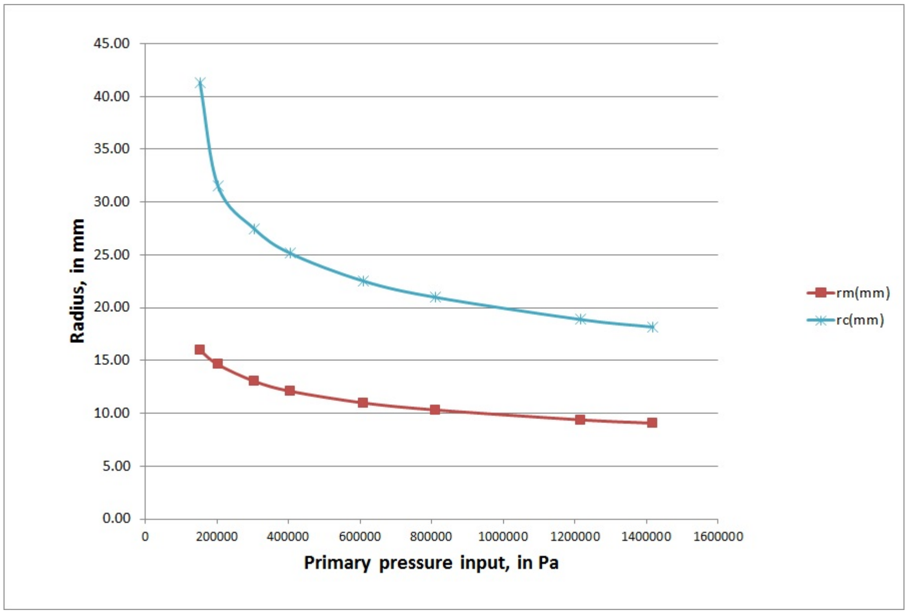

Figure 4.3: The mixing chamber radius and ejector exit radius for 300K primary inlet

The fact that recoverable pressure at the exit of the ejector will go on increasing with primary inlet pressure is shown in Fig.4.4.

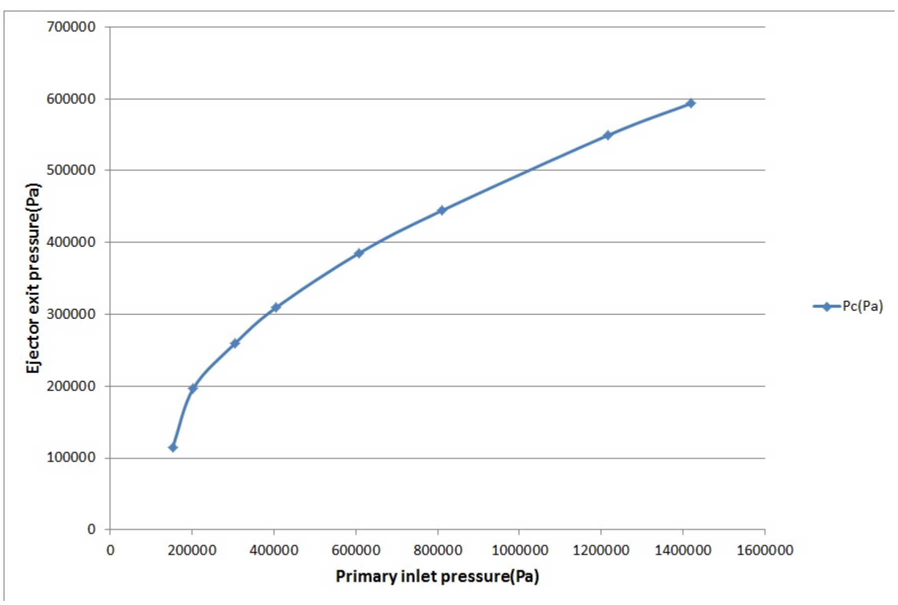

Figure 4.4: Exit pressure of ejector for 300K primary inlet

4.2 Ejector Design for 150K Primary Flow Inlet

Ejector design by segmentation approach is applied for 150K primary inlet with different pressures, which gives geometrical parameters as described below. The purpose of the calculations for ejector design parameters at different pressure and temperature range is to explore the variation of ejector size in different ranges and to check its deviation for the range of parameters.

P_g(Pa)	r_t(mm)	r_{p1}(mm)	T_{p1}(K)	r_1(mm)	r_m(mm)	r_c(mm)	P_c(Pa)
1418550	4.16	6.38	45.05	10.59	7.27	14.56	631254
1215900	4.49	6.62	47.91	10.74	7.56	15.18	580197
810600	5.50	7.34	56.34	11.20	8.37	16.99	462376
607950	6.95	8.31	68.36	11.86	9.39	18.33	397056
405300	7.77	8.90	74.32	11.34	9.25	20.56	315271
303975	8.98	9.73	83.38	12.89	10.71	22.56	261808
202650	10.99	11.23	98.05	14.06	12.06	26.01	196913
151988	12.69	12.70	110.01	15.25	13.22	34.30	113143

Table 4.2: Ejector design for 150K primary inlet and mass flow rate of 100 gps

The variation in the geometry of the ejector for the range of pressure from 1.5 bar to 14 bar has been shown in Fig.4.5, Fig.4.6, Fig.4.7.

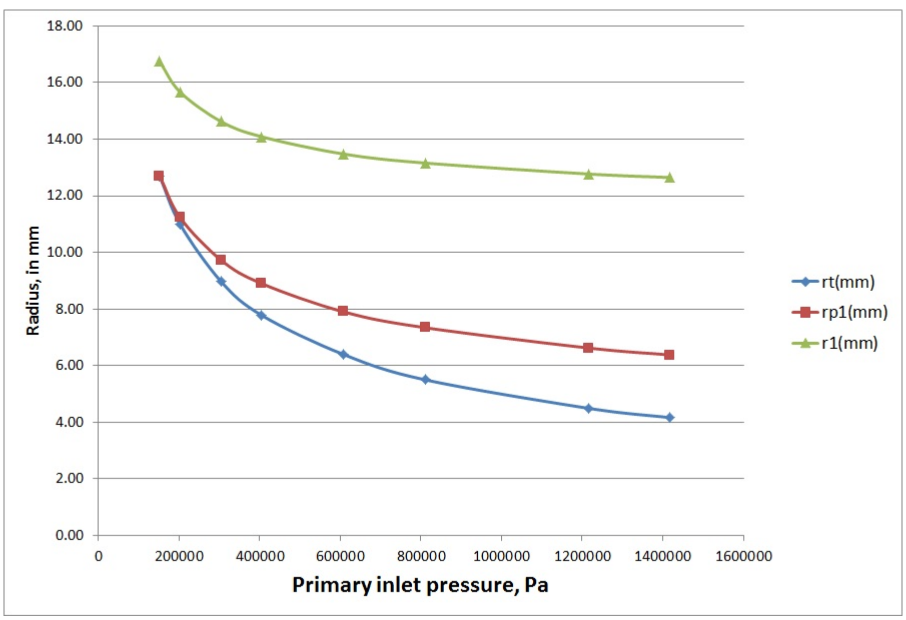

Figure 4.5: Primary nozzle throat radius,primary nozzle exit radius and convergent portion inlet radius for 150K primary inlet

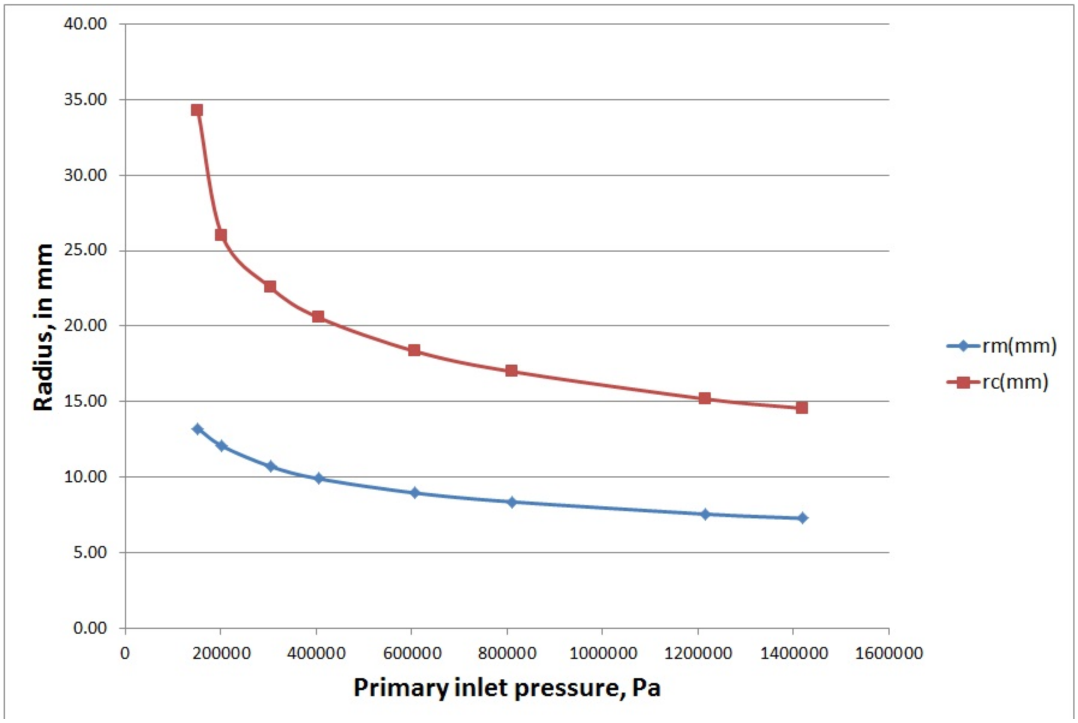

Figure 4.6: Mixing chamber radius and ejector exit radius for 150K primary inlet

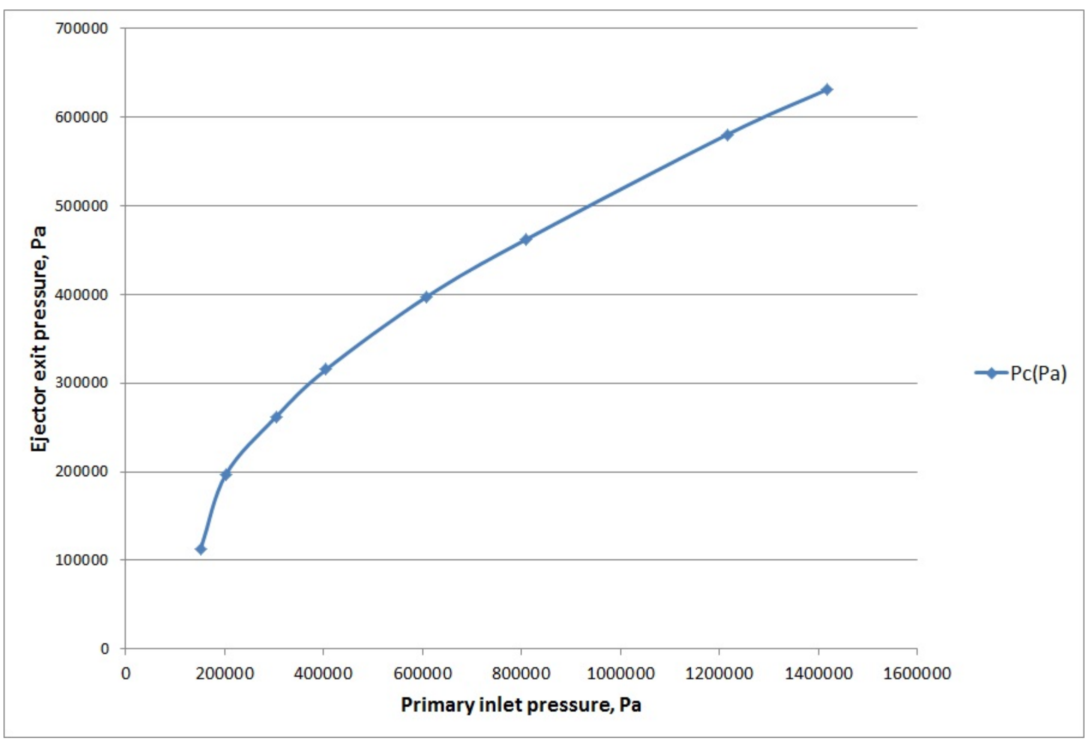

Figure 4.7: Exit pressure of ejector for 150K primary inlet

4.3 Ejector Design for 10K Primary Inlet

Ejector design by segmentation approach is applied for 10K primary inlet with different pressures, which gives geometrical parameters as described in table 4.3 and Fig. 4.8, Fig. 4.9 and Fig. 4.10.

P_g(Pa)	r_t(mm)	r_{p1}(mm)	T_{p1}(K)	r_1(mm)	r_m(mm)	r_c(mm)	P_c(Pa)
1215900	2.024	3.100	3.851	5.202	3.438	8.554	367269
810600	2.587	3.433	3.851	5.408	3.733	9.380	325432
607950	3.042	3.740	4.142	5.608	3.949	9.990	298741
405300	3.796	4.339	0.000	6.024	4.277	10.895	261338
303975	4.431	4.791	5.486	6.357	4.732	11.979	220049
202650	5.481	5.595	6.490	6.984	5.511	13.710	170842
151988	6.360	6.363	7.303	7.610	6.422	15.478	135124

Table 4.3: Ejector design for 10K primary inlet and mass flow rate of 100 gps

The ejector design proposed here, is to be installed at working parameters in the range 10K, so it is crucial to know the behavior of the gas at this very low temperature range.

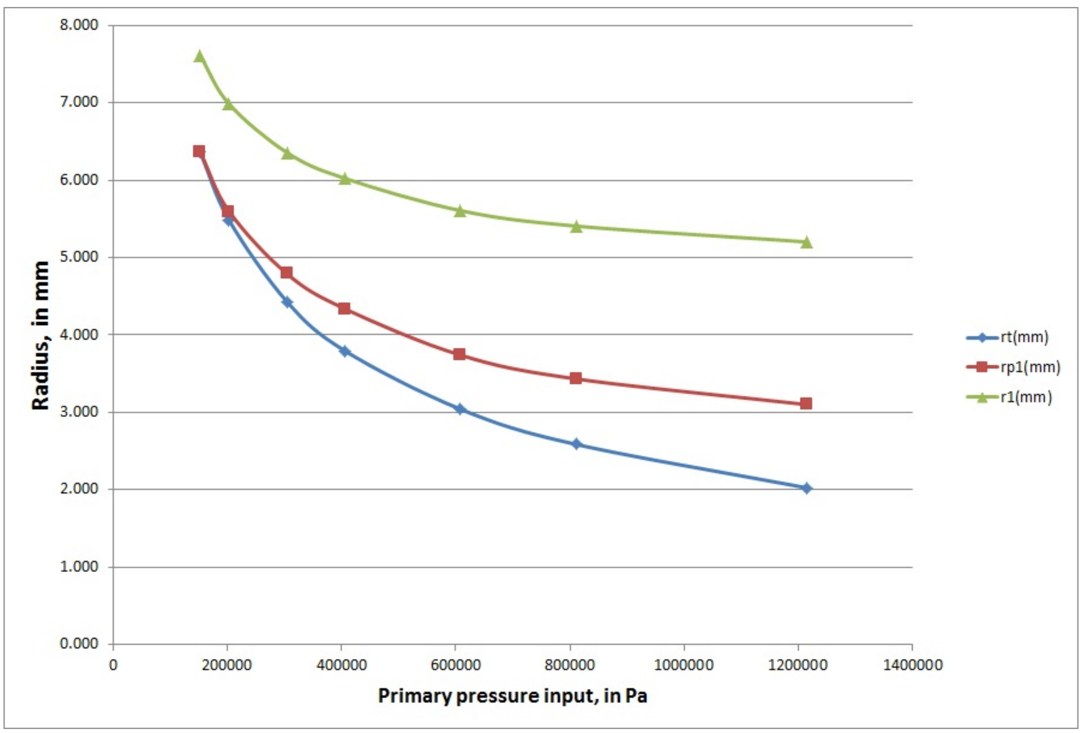

Figure 4.8: Nozzle throat radius,Nozzle exit radius and convergent portion inlet radius for 10K primary inlet

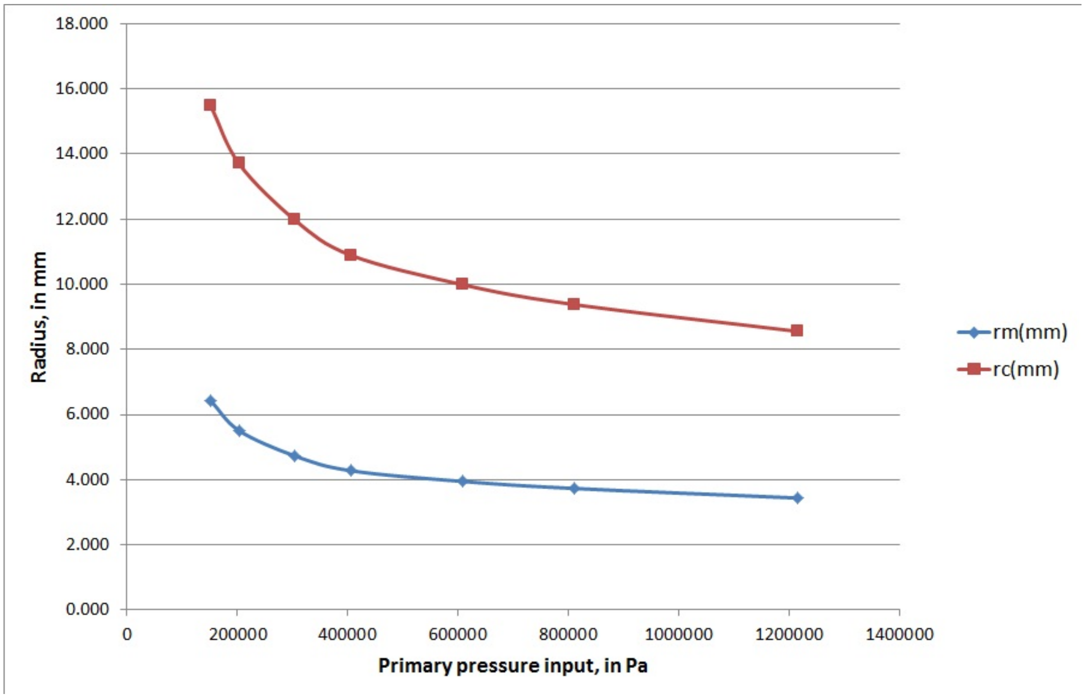

Figure 4.9: Mixing chamber radius and ejector exit radius for 10K primary inlet

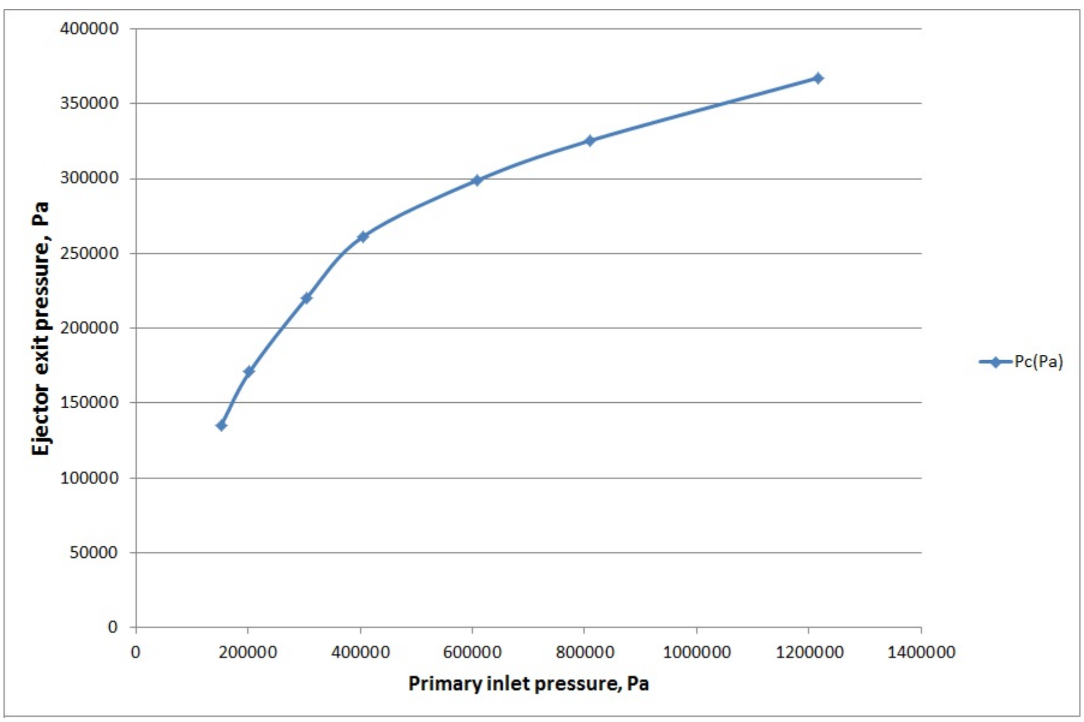

Figure 4.10: Exit pressure of ejector for 10K primary inlet

4.4 Comparison between Geometrical Parameters of Ideal Gas Modeling and Real Gas Modeling

Requirement of development of new approach for design of ejector arose due to non ideal gas behavior of Helium in the range of working temperature of less than 10K.

The comparison of results of ideal gas modeling and real gas modeling is essential to know the improvement of results achieved.

T_g(K)	r_t(mm)	r_{p1}(mm)	T_e(K)	r_1(mm)	r_m(mm)	P_c(Pa)	T_c(K)
300	9.37	10.73	150	22.98	17.24	123971	174.72
200	8.47	9.69	100	20.76	15.58	123971	116.48
100	7.12	8.15	50	17.46	13.10	123971	58.24
50	5.99	6.85	25	14.68	11.02	123971	29.12
20	4.76	5.45	10	11.67	8.76	123971	11.65
10	4.00	4.58	5	9.82	7.37	123971	5.82

Table 4.4: Results of ejector parameters for ideal gas modeling

These results in table 4.4 and 4.5 are for the primary stream at 100gps and 4 bar and secondary stream at 80 kPa.

T_g(K)	r_t(mm)	r_{p1}(mm)	T_e(K)	r_1(mm)	r_m(mm)	P_c(Pa)	T_c(K)
300	9.242	10.581	150	22.911	14.104	194439.81	209.562
200	8.352	9.561	100	20.704	12.727	194972.38	139.566
100	7.026	8.040	50	17.412	10.657	196601.74	69.576
50	5.908	6.755	25	14.637	8.877	200460.15	34.593
20	4.671	5.329	10	11.567	6.802	217897.43	13.674
10	3.796	4.327	5	11.141	5.911	224273.54	8.103

Table 4.5: Results of ejector parameters for real gas modeling

Deviatoin in the results of real gas modeling are shown in graph below.

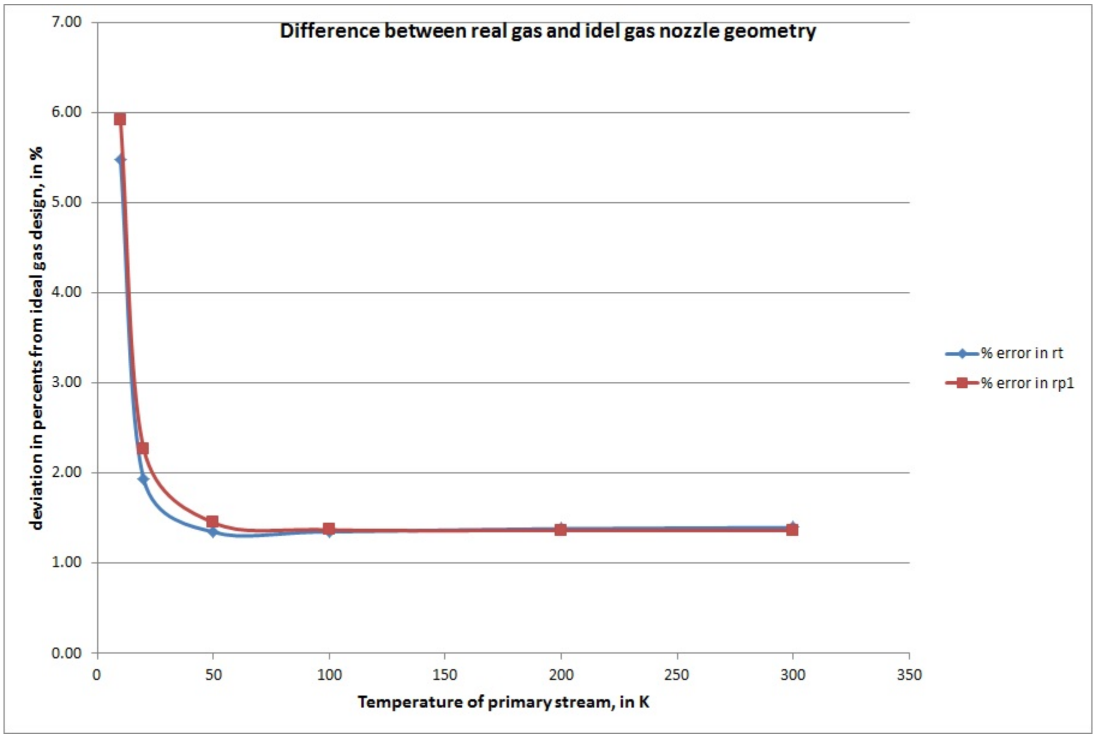

Figure 4.11: Deviation in throat radius and nozzle exit radius for real gas modeling with respect to ideal gas modeling

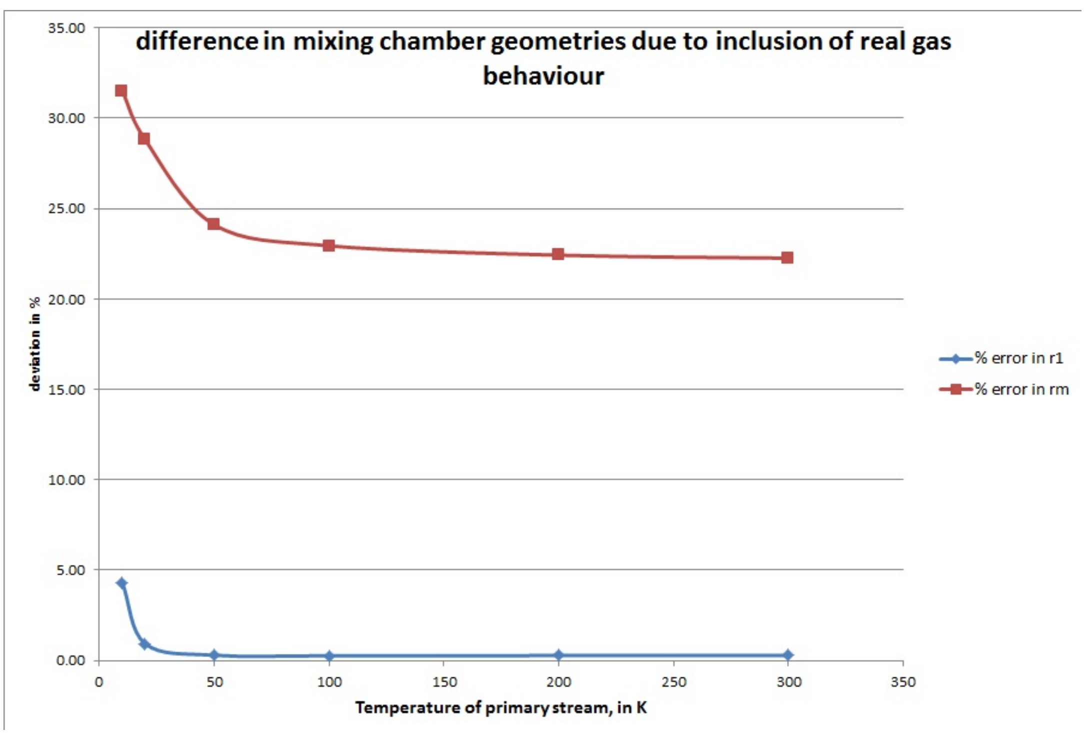

Figure 4.12: Difference in mixing chamber entrance radius and constant area duct radius due to inclusion of real gas behavior

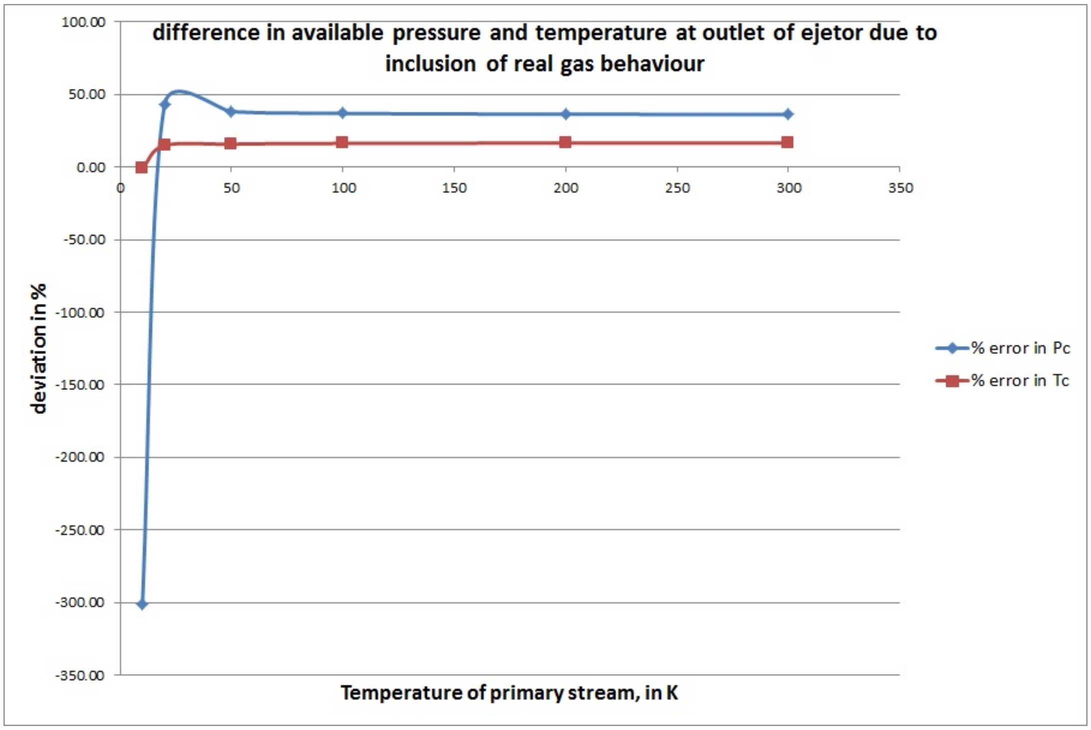

Figure 4.13: Difference in available pressure and temperature at outlet of ejector between real gas Modelling and ideal gas modelling

Significant deviations in design results are observed as shown in Fig. 4.11, Fig.4.12 and Fig. 4.13 due to real gas modeling, particularly at working of cryogenic temperature range. This highlights the importance and inevitability of real gas modeling in the cryogenic temperature range.Furthermore, the numerical simulation of this real gas modeling is done in subsequent sections.

Chapter 5

Computational Fluid Dynamics Simulation for Helium Ejector

Different commercial softwares are being used in the design and analysis processes which saves time and cost of new design, but also are used to study systems where experimental investigation is difficult or impossible to perform.

In the area of fluid dynamics, there are number of commercial computational fluid dynamics (CFD) packages available for modeling flow structure in or around objects. Combined with the use of test data, CFD can be used in the design process to drive geometry change instead of being used mainly as a design validation tool.

One of the most critical requirements for any CFD tool used for thermal applications is the ability to simulate flows along nozzles, turbines. Such challenging features as pressure gradients, shocks, velocity distribution, eddy location, stream line curvature, and stream wise vortexes pose a challenge for computation.

The small margins of improvement that are usually targeted in nozzle and turbines design today require precise tools capable of discerning small differences between alternative designs.

Custom modeling tools that are based as simplified numerical methods and assumptions cannot provide the accuracy that can be obtained with CFD, which offers mainly inherent advantages for e.g.: it offers quick and cheap solutions in comparison to experimental solutions and more accurate in comparison to empirical methods used in design. Accurate simulation of flows through the nozzle is important for prediction of velocity pattern and pressure patterns.

5.1 CFD Simulation of Ejector Designed According to Novel Design Procedure

Ejector with 4 bar and 10K primary Helium fluid has been designed to suck the 0.8bar and 10K secondary helium fluid. Which gives 201kPa and 7.76K temperature outlet.

Numerical simulation of ejector has been done as pressure inlet boundary condition for primary and secondary inlet and pressure outlet boundary condition for outlet. k-ϵ RNG model in Fluent of ANSYS 14.5, which is suggested for ejector by overwhelming majority of the researchers.

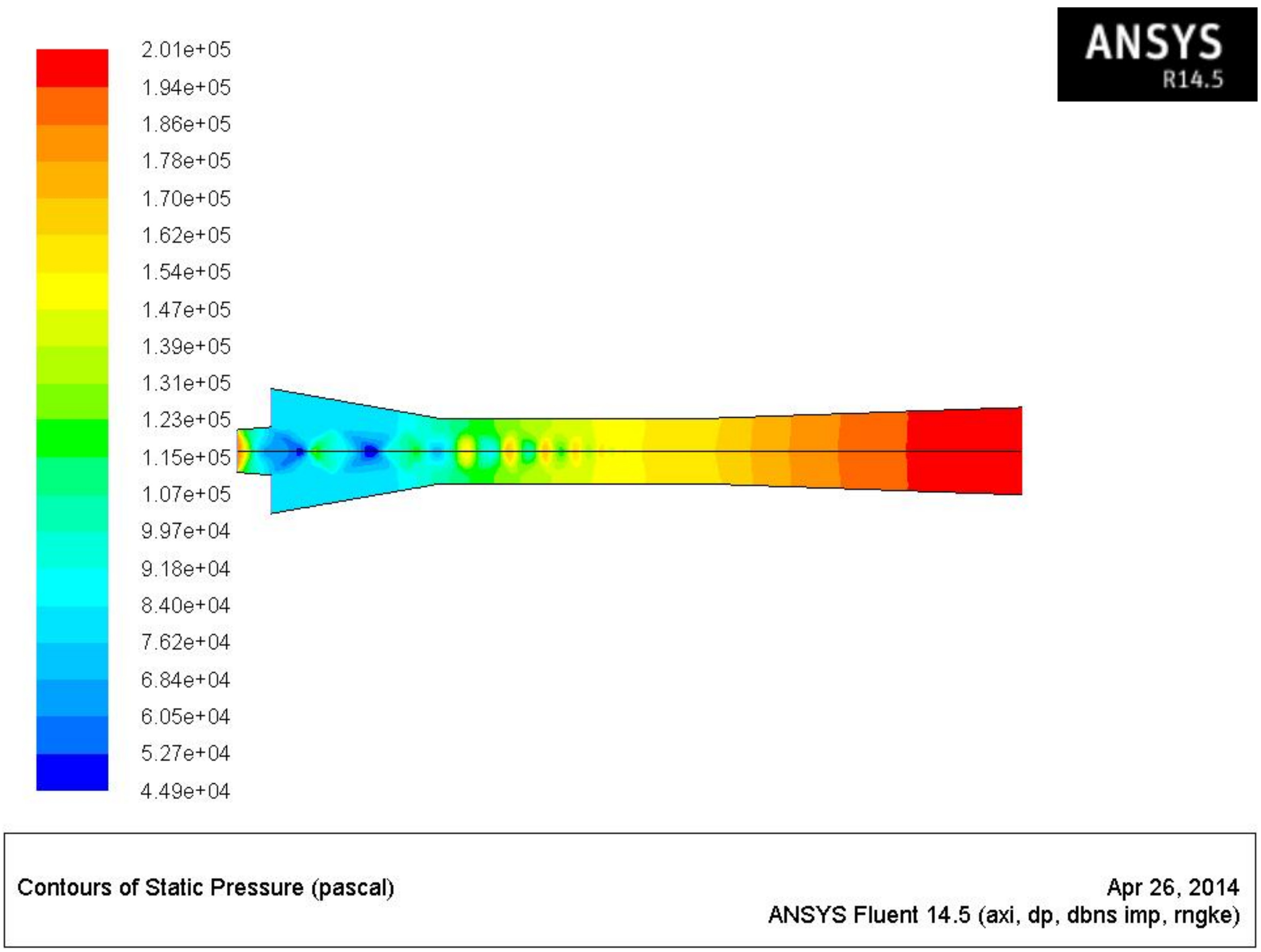

Figure 5.1: Pressure distribution in ejector for 10K primary inlet with 10 degree convergent angle

The NIST real gas modeling has been used to include helium,which is available in the density-based solvers. They use the National Institute of Standards and Technology (NIST) Thermodynamic and Transport Properties of Refrigerants and Refrigerant Mixtures Database

(REFPROP) to evaluate thermodynamic and transport properties of approximately pure fluids or a mixture of these fluids. The REFPROP database is a shared library that is dynamically loaded into the solver when you activate one of the NIST real gas models in a FLUENT session. Once the NIST real gas model is activated, control of relevant property evaluations is relinquished to the REFPROP database, and any information for a fluid that is displayed in the Materials panel is ignored by the solver. However, all postprocessing functions will properly report and display the current thermodynamic and transport properties of the real gas.

The convergence angle has been taken as 10 degree and mixing chamber length as 50mm.Solution converged in 3613 iterations. The result of simulation in terms of pressure distribution and Mach No are shown in Fig.5.1 and Fig.5.2.

The pressure shown by this simulation is quite similar to the shock train in the experimental investigation of the typical ejectors in the literature. This implies that k-ϵ RNG model of turbulence is good enough for simulation of ejector under custody.

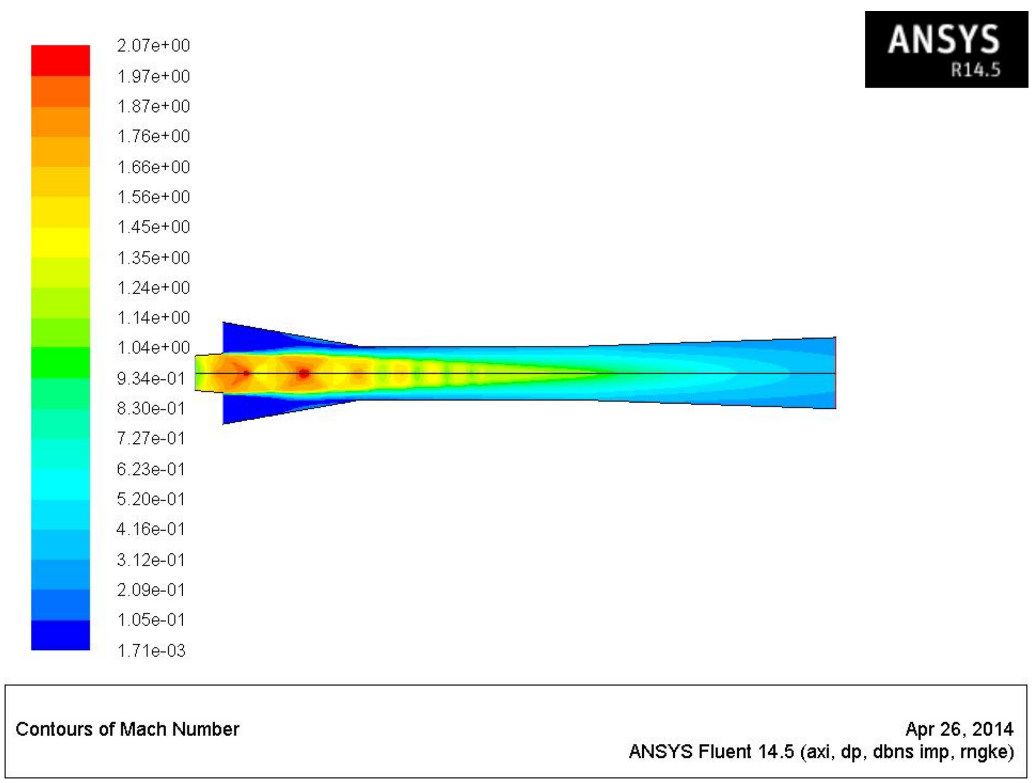

Figure 5.2: Mach No variation in ejector for 10K primary inlet with 10 degree convergent angle

This simulation yields the mass flow rate of secondary fluid 6.13 gps for 100 gps of primary Helium flow.

5.2 Grid Independence Check for the Helium Ejector

Maximum face size of mesh has been varied from 1 mm to 0.1 mm and simulation has been carried out for the range of maximum face sizes. Ejector with 4 bar and 10K primary Helium fluid has been designed to suck the 0.8bar and 10K secondary helium fluid. Which gives 201kPa and 7.76K temperature outlet.

Numerical simulation of ejector has been carried as pressure inlet boundary condition for primary and secondary inlet and pressure outlet boundary condition for outlet. k-ϵ RNG turbulence model in Fluent 14.5, which is suggested for ejector by overwhelming majority of the researchers.

The results of the grid independence check are shown in table 5.1.

No. of Nodes	No. of elements	Max. Face size(mm)	No. of Iterations	Entrainment Ratio
1014	874	1	554	0.057
1603	1429	0.8	660	0.061
2672	2442	0.6	1050	0.067
5834	5487	0.4	1630	0.081
14499	13947	0.25	3247	0.086
22467	21779	0.2	4250	0.087
27520	26757	0.18	4882	0.087
39506	38583	0.15	6223	0.086
52349	51288	0.13	7484	0.086
72733	71476	0.11	9284	0.086
87579	86200	0.1	10500	0.086

Table 5.1: Grid independence check for helium ejector

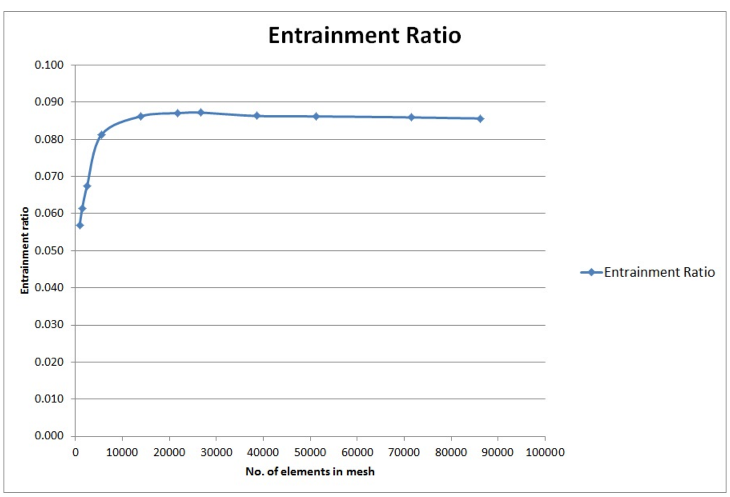

Figure 5.3: No. of elements v/s entrainment ratio

It is evident from Fig.5.3 that grid maximum face size of 0.25 mm is good enough to predict the flow field independent of no. of elements in mesh.

5.3 Optimization of Convergent Angle of the Helium Ejector

The ejector design with primary helium at 4 bar and 10K and secondary helium at 80kPa and 10K yields in outlet at 201.6kPa pressure and 7.76K temperature.

The convergent angle optimization has been done through CFD analysis using Fluent 14.5 for angle of 5 degree to 50 degree.

pressure distribution results for some the convergent angles are presented here.

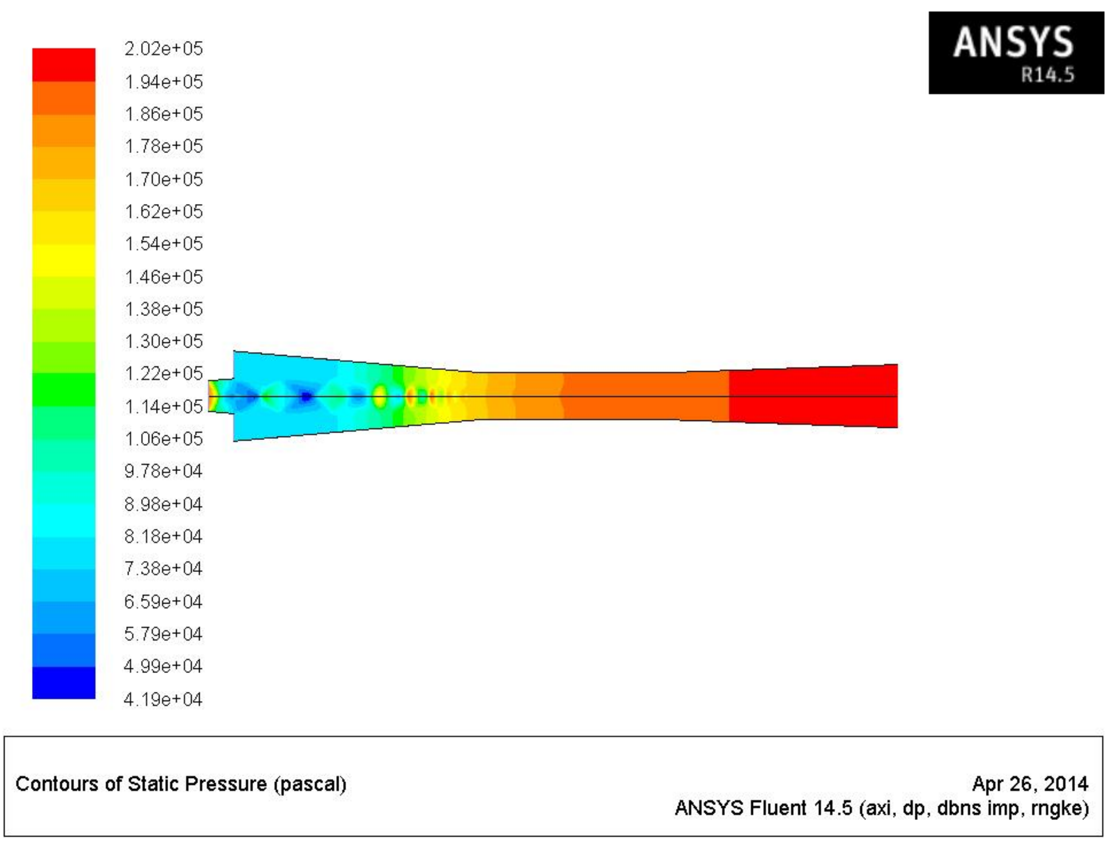

Figure 5.4: The pressure distribution pattern for the helium ejector with 5 degree convergent angle

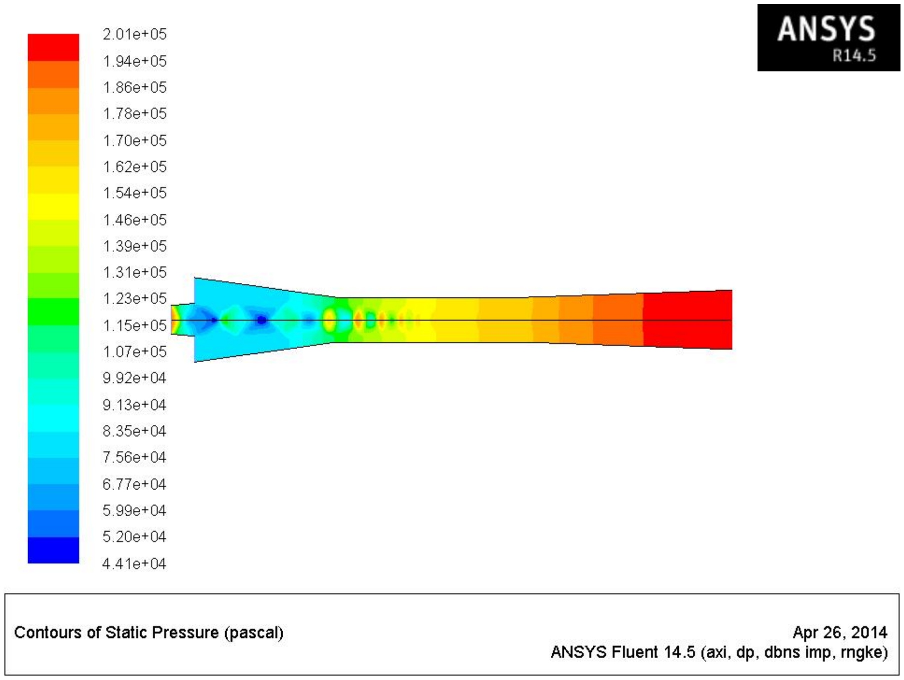

Figure 5.5: The pressure distribution pattern for the helium ejector with 8 degree convergent angle

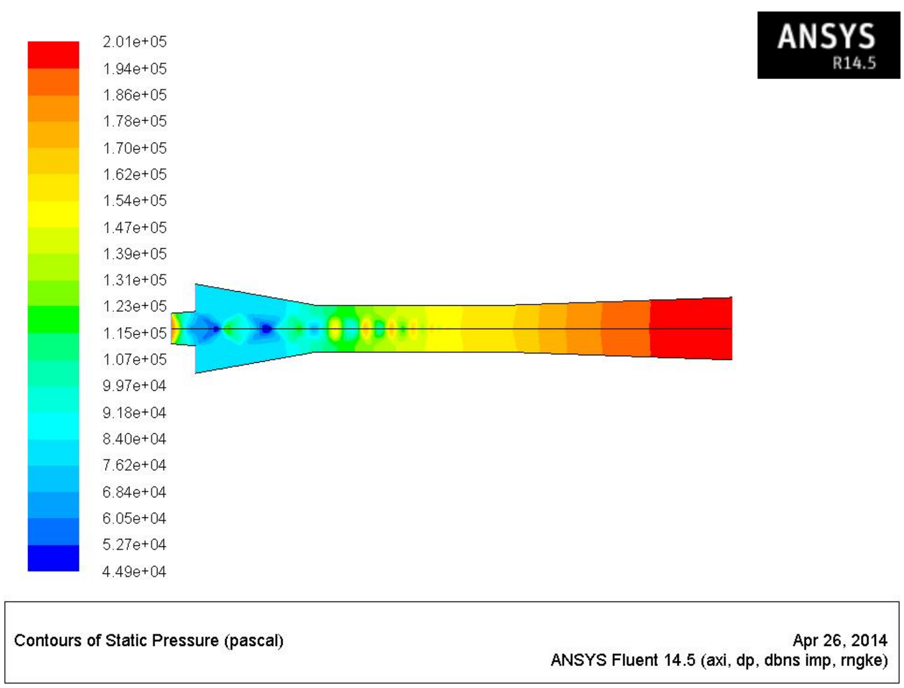

Figure 5.6: The pressure distribution pattern for the helium ejector with 10 degree convergent angle

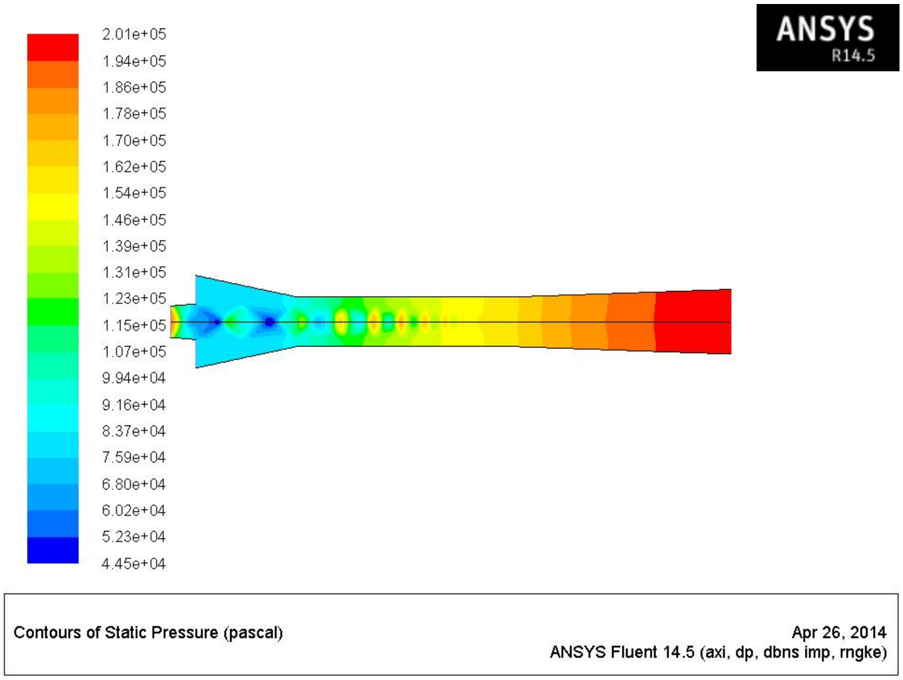

Figure 5.7: The pressure distribution pattern for the helium ejector with 12 degree convergent angle

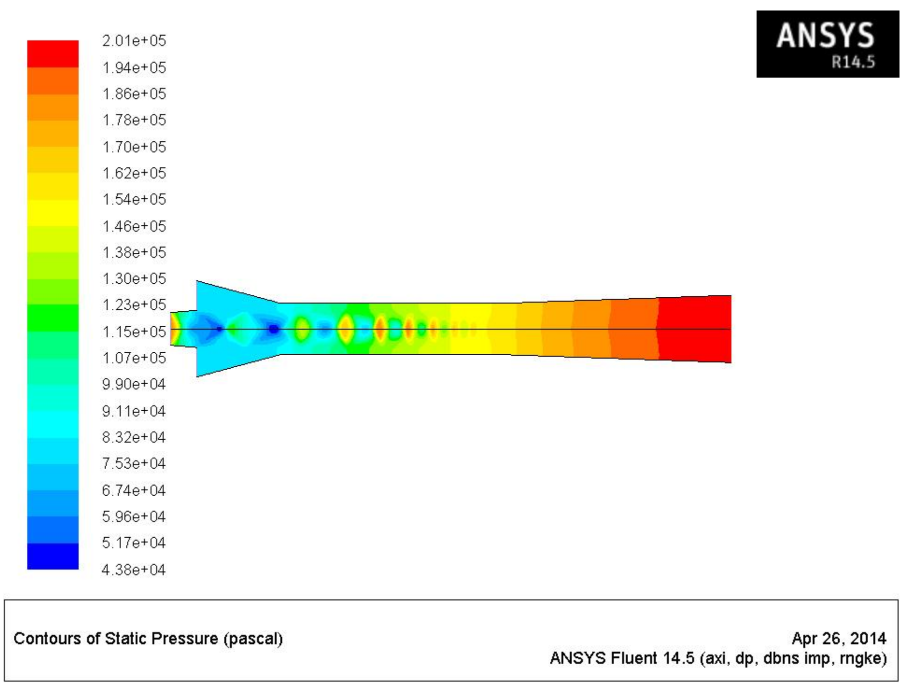

Figure 5.8: The pressure distribution pattern for the helium ejector with 15 degree convergent angle

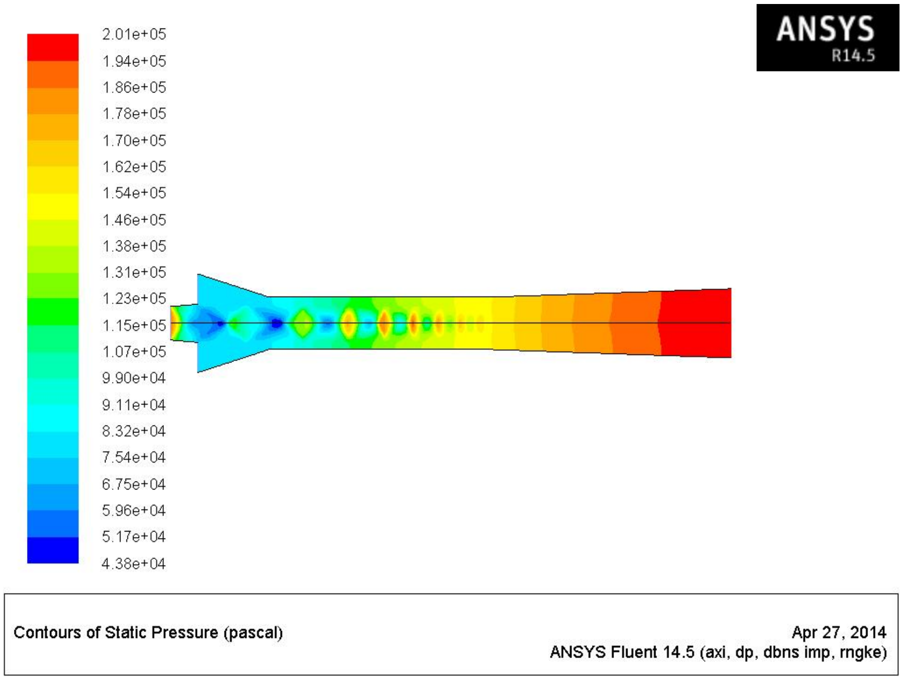

Figure 5.9: The pressure distribution pattern for the helium ejector with 18 degree convergent angle

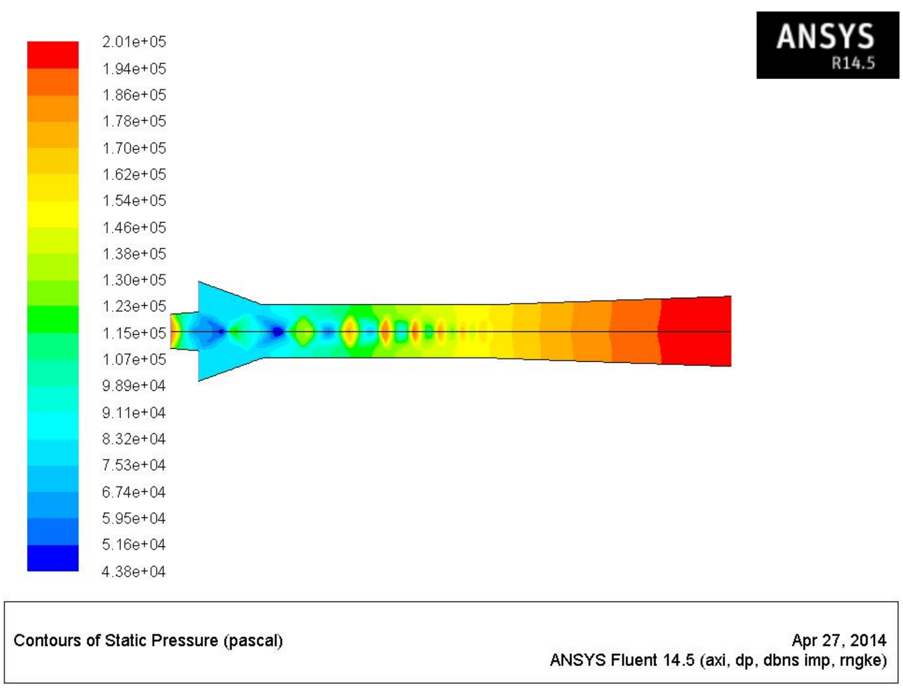

Figure 5.10: The pressure distribution pattern for the helium ejector with 20 degree convergent angle

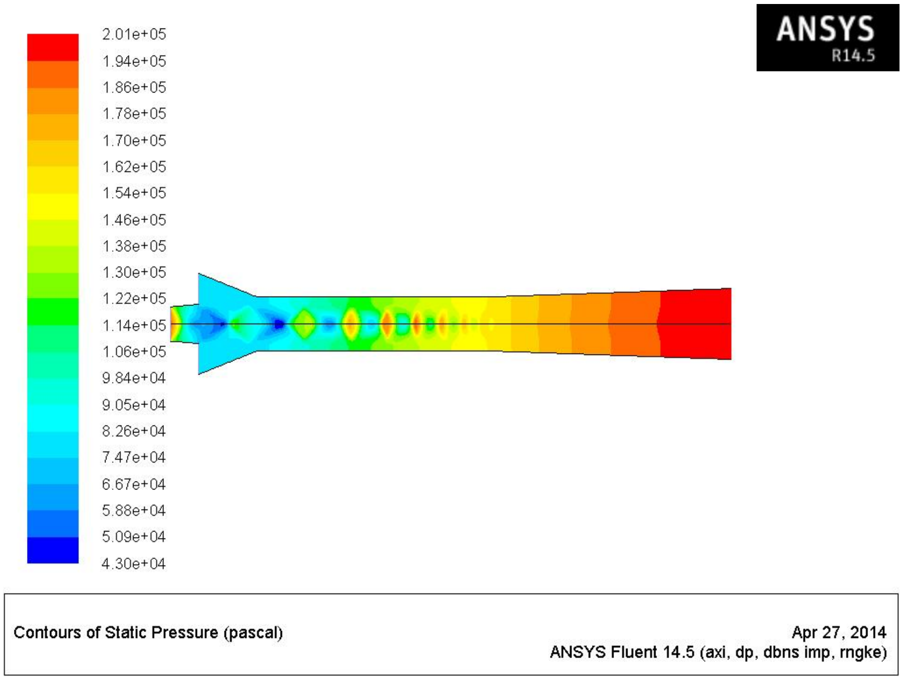

Figure 5.11: The pressure distribution pattern for the helium ejector with 22 degree convergent angle

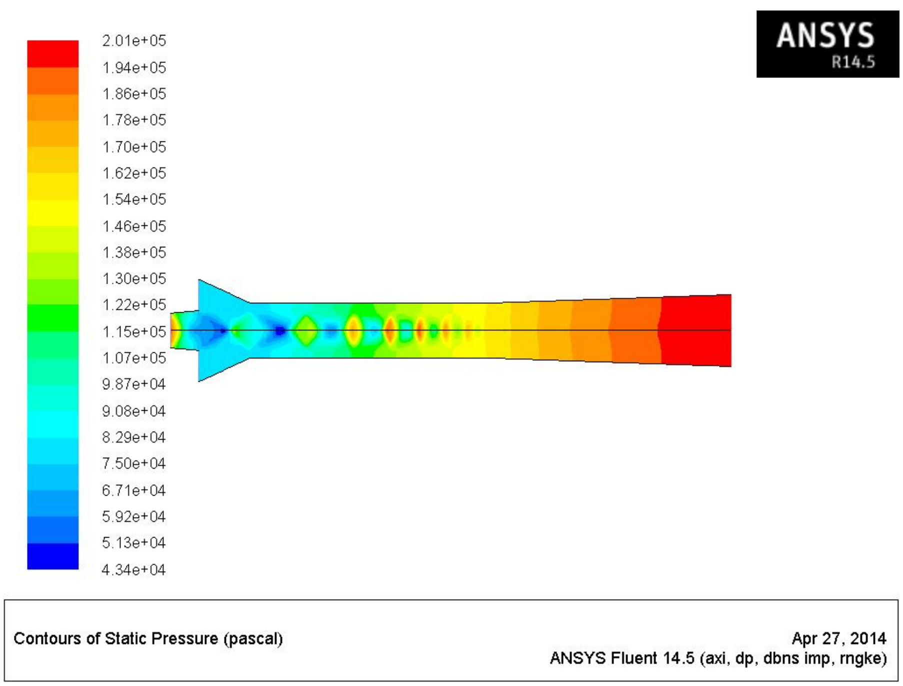

Figure 5.12: The pressure distribution pattern for the helium ejector with 25 degree convergent angle

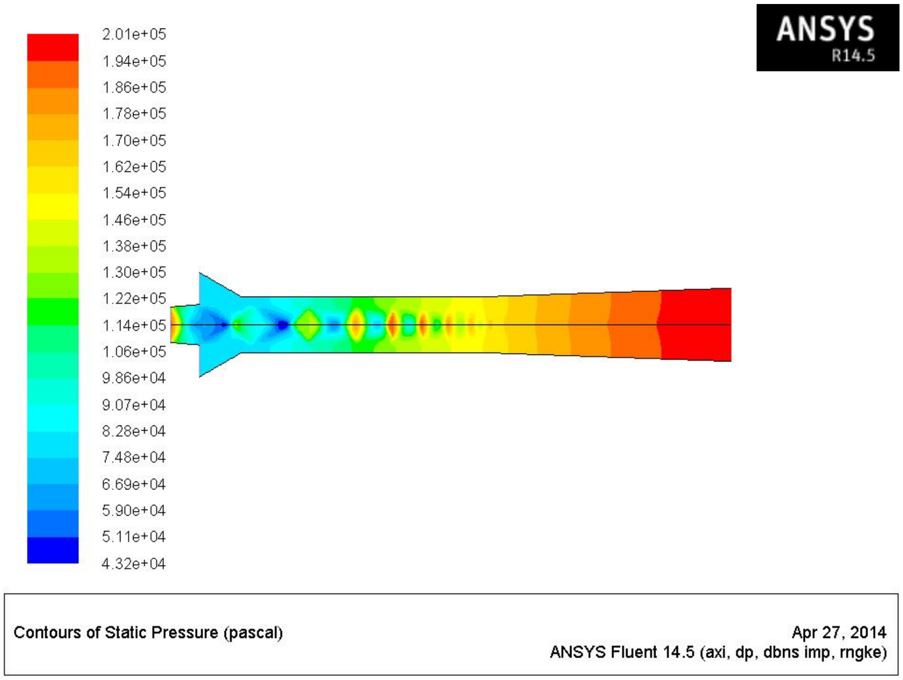

Figure 5.13: The pressure distribution pattern for the helium ejector with 30 degree convergent angle

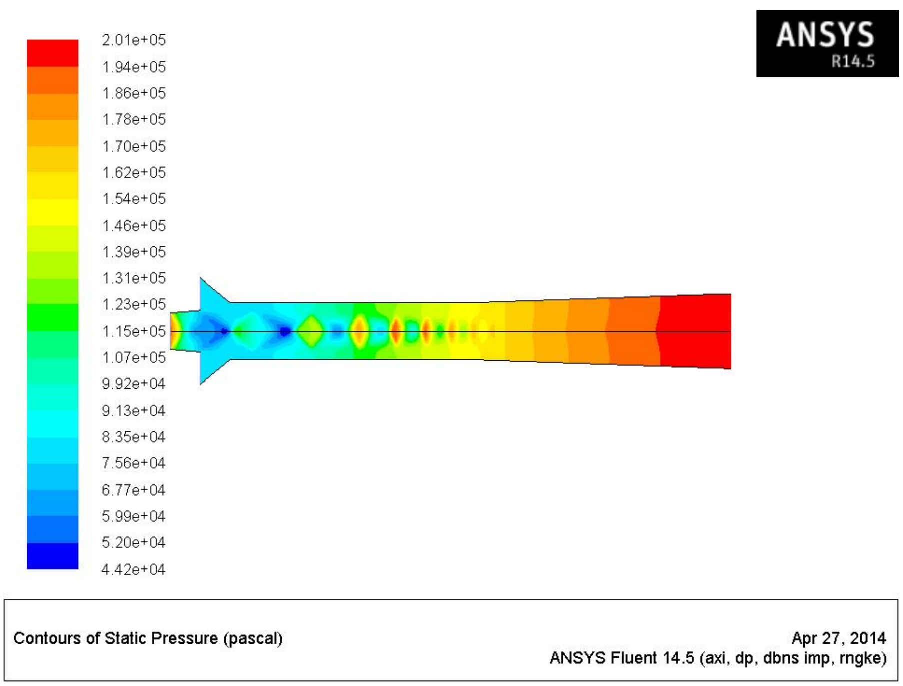

Figure 5.14: The pressure distribution pattern for the helium ejector with 40 degree convergent angle

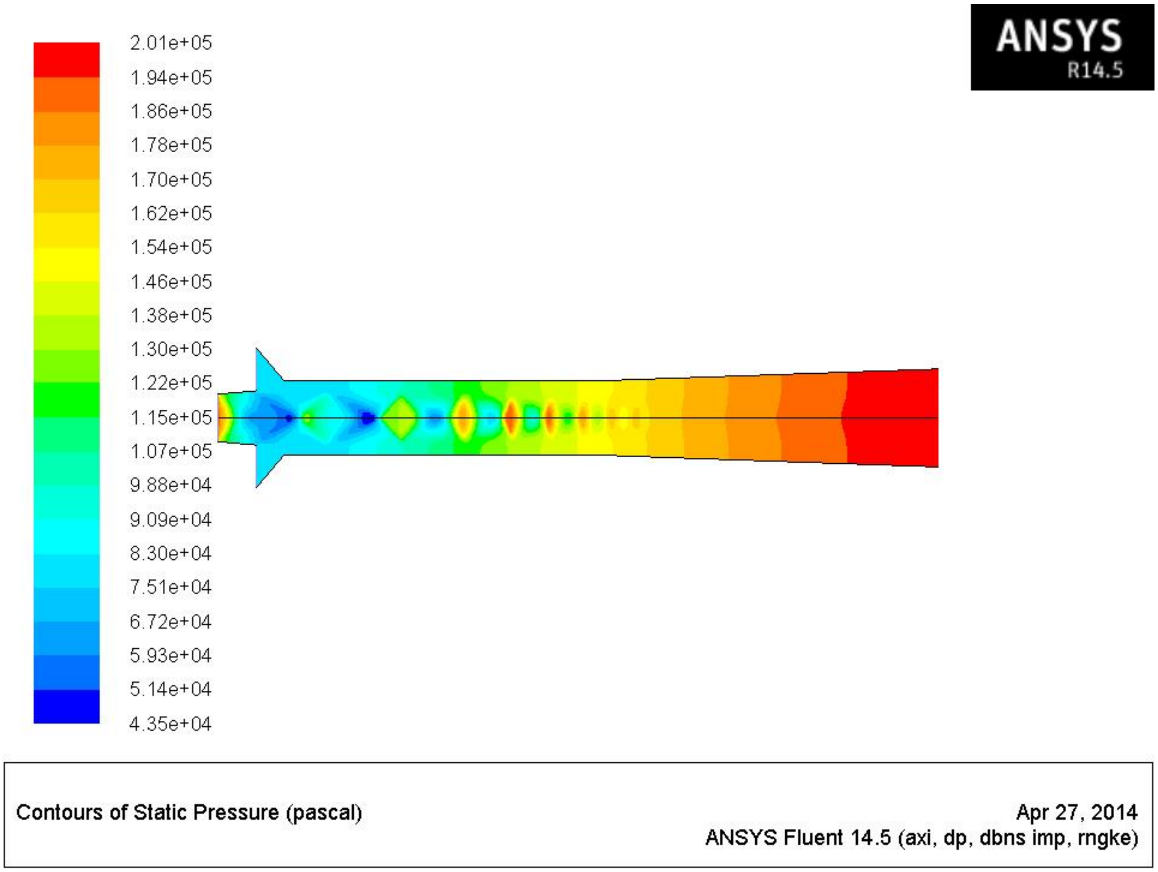

Figure 5.15: The pressure distribution pattern for the helium ejector with 50 degree convergent angle

Convergent Angle	Primary mfr(gps)	Secondary mfr(gps)	Entrainment ratio
5	99.986	-28.437	-0.284
8	99.986	1.812	0.018
10	99.986	6.126	0.061
12	99.986	8.143	0.081
15	99.986	8.623	0.086
18	99.986	8.387	0.084
20	99.986	8.081	0.081
22	99.986	7.841	0.078
25	99.986	7.496	0.075
30	99.986	7.095	0.071
40	99.986	6.831	0.068
50	99.986	6.408	0.064

Table 5.2: CFD results of mass flow rates for different convergent angles of the ejector

The pressure distribution and corresponding entrainment for different convergent angles clearly shows that shock train inside the constant area chamber is beneficial for the entrainment of secondary fluid.

Furthermore, 15 degree convergent angle comes out as optimum for given configuration. Graph shown below describes it more evidently.

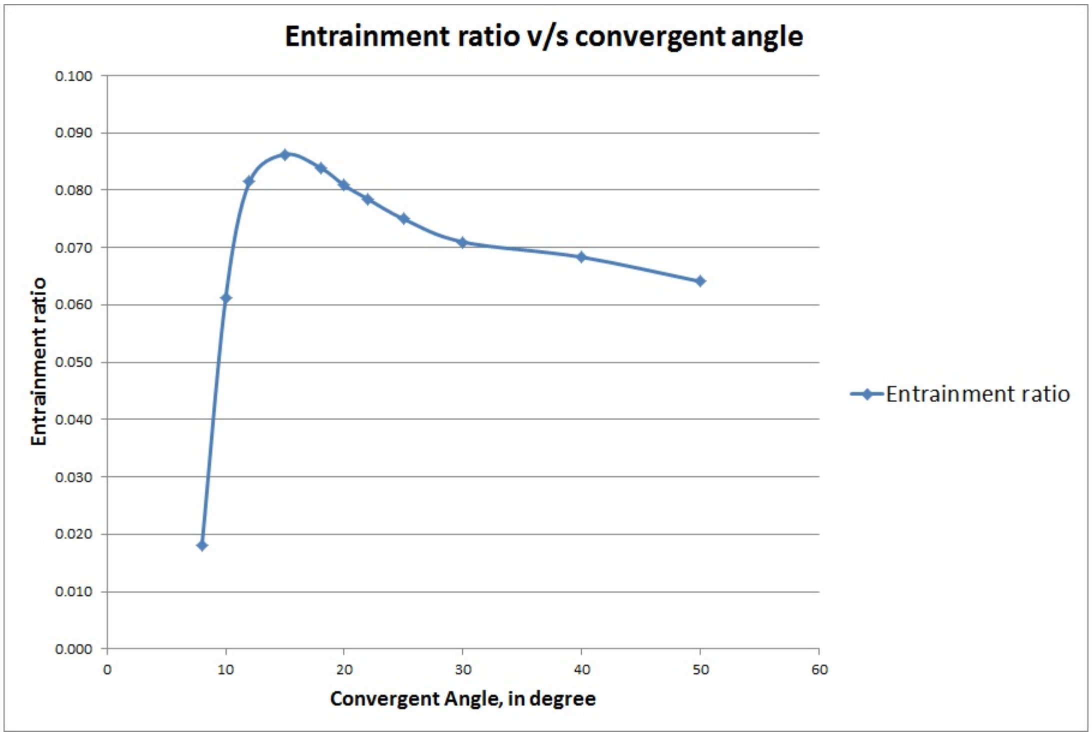

Figure 5.16: Entrainment ratio v/s convergent angle of mixing chamber

5.4 Optimization of Constant Area Duct Diameter

Constant area duct diameter is important parameter in ejector design considerations as it decides the mixing pressure of the primary and secondary stream, which eventually effects the entrainment capacity of ejector.

To represent the effect of constant area duct on ejector performance in non-dimensional terms its area is divided by throat area of primary nozzle, which makes it easier to compare the ejectors with different configurations.

Numerical simulation has been done for the range of diameters of constant area duct to find the area where the entrainment is maximum. Results of numerical simulations for the diameters from 5.2 mm to 6.2 mm are tabulated below.

constant area duct diameter, in mm	Area of constant area duct, A3(mm2)	$\frac{A_3}{A_t}$	Secondary flow inlet, in gps	Entrainment ratio
5.200	21.226	1.877	8.218	0.082
5.400	22.891	2.024	11.112	0.111
5.600	24.618	2.176	12.727	0.127
5.800	26.407	2.335	10.249	0.103
5.911	27.428	2.425	8.623	0.086
6.000	28.260	2.498	7.079	0.071
6.200	30.175	2.668	3.198	0.032

Table 5.3: Variation of entrainment ratio with change in constant area duct diameter

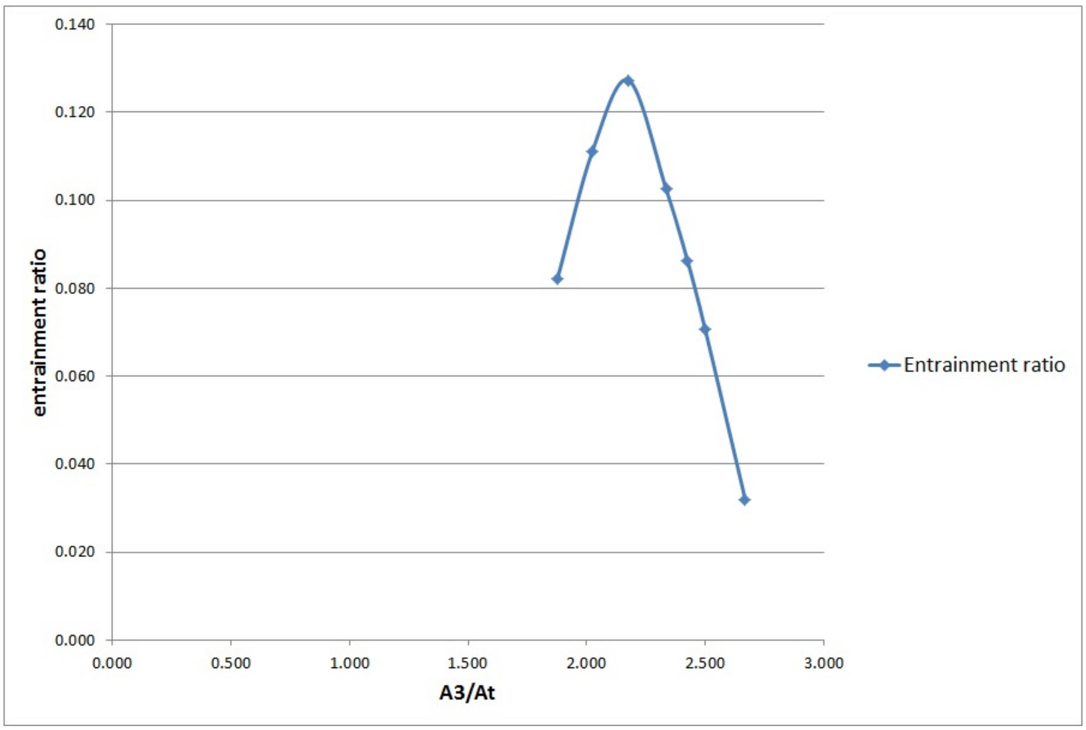

Figure 5.17: Change of entrainment ratio with change in constant area duct diameter

The results of CFD simulation of varying constant area duct diameter show that 5.6 mm diameter of the same give optimum entrainment that leads to the selection of duct diameter as 5.6 mm.

Chapter 6

Conclusions and Future Work

In the present study, 1-D analysis for the prediction of the ejector performance has been carried out at critical mode operation. The constant-pressure mixing has been assumed occurring inside the constant-area section of the ejector and the entrained flow at choking condition is analyzed. However, this analytical ideal gas modelling approach assumes the specific heat and adiabatic ratio of fluid, which is not the case.

So a novel approach based on real gas properties has been deployed, which eliminates the requirement of specific heat and heat ratio in calculation of flow behavior.Software HEPACK is used to get real gas properties at segmented flow using MS EXCEL. This leads to a considerably convenient approach for ejector design.

Furthermore, this analytical model has been validated by numerical simulation in ANSYS 14.5 Fluent using turbulence modeling. Certain parameters like convergent angle and mixing chamber length are optimized through CFD.

The conclusions which can be drawn from this work are:

1. The ejector has supersonic operational conditions as it is required to produce very low pressure at exit of nozzle to suck the secondary flow and produce partial vacuum in the small Dewar, so a convergent-divergent primary nozzle is required.

2. The primary jet of Helium at 4 bar is able to suck the secondary flow of Helium at 0.7 bar with a entrainment ratio of 0.12 according numerical simulation carried out in this study for optimized design.

3. Both the pressure ratio and the entrainment ratio are dependent upon the primary stream mass flow rate and the J-T valve restriction.

4. A novel approach for the analytical design using real gas properties is quite consistent with CFD analysis with inclusion of helium properties using REFPROP in Fluent 14.5,

which implies that the proposed design methodology is viable alternative for the design of the ejector.

5. Certain parameters of ejector has been optimized using numerical simulation, which indicates that the optimum convergent angle for mixing chamber is15^o and the optimum radius of mixing chamber is 5.2 mm for given configuration.

The present work can be extended as follows:

1. Numerical simulation of ejector has been carried out in this study. However, for performance analysis of ejector it would be advisable to investigate the design experimentally for assurance.

2. To capture the flow field behavior of further low temperature fluid, it would require to use more refined numerical tools for assessment of phase change phenomenon.

Bibliography

[1] Dandachi, Jaber M.A., Steam air ejector performance and its dimensional parameters, PhD thesis, Loughborough University Of Technology (1990)

[2] Jose M. Cardemil, Sergio Colle, ”A general model for evaluation of vapor ejectors performance for application in refrigeration”, Energy Conversion and Management, Volume 64(2012)

[3] Yahya S.M., ”Fundamentals of Compressible Fluid Flow”, 4th ed., New Age Intl. Publishers (2012)

[4] Johnson D. L., Daggett D. L., ”A Cold Ejector for Closed-Cycle Helium”, TDA Progress Report (1987)

[5] Chen WeiXiong, Ming Liu, DaoTong Chong, JunJie Yan, Adrienne Blair Little, Yann Bartosiewicz, A ”1D model to predict ejector performance at critical and sub-critical operational regimes”, International Journal of Refrigeration, Volume 36, Issue 6, (2013)

[6] Huang B.J., Chang J.M., Wang C.P., Petrenko V.A., ”A 1-D analysis of ejector performance” International Journal of Refrigeration (1999)

[7] Cui Li, Yanzhong Li, Lei Wang, ”Configuration dependence and optimization of the entrainment performance for gas-gas and gas-liquid ejectors”, Applied Thermal Engineering, Volume 48 (2012)

[8] Yadav Randheer L., Patwardhan Ashwin W., ”Design aspects of ejectors: Effects of suction chamber geometry”, Chemical Engineering Science, Volume 63, Issue 15 (2008)

[9] Hisham El-Dessouky, Hisham Ettouney, Imad Alatiqi, Ghada Al-Nuwaibit, ”Evaluation of steam jet ejectors”, Chemical Engineering and Processing: Process Intensification, Volume 41, Issue 6 (2002)

[10] Yinhai Zhu, Wenjian Cai, Changyun Wen, Yanzhong Li, "Numerical investigation of geometry parameters for design of high performance ejectors", Applied Thermal Engineering, Volume 29, Issues 5-6 (2009)

[11] Huang B.J, Chang J.M, "Empirical correlation for ejector design", International Journal of Refrigeration, Volume 22, Issue 5 (1999)

[12] Sriveerakul T., Aphornratana S., Chunnanond K., "Performance prediction of steam ejector using computational fluid dynamics: Part 1. Validation of the CFD results", International Journal of Thermal Sciences, Volume 46, Issue 8 (2007)

[13] Yinhai Zhu, Wenjian Cai, Changyun Wen, Yanzhong Li, "Simplified ejector model for control and optimization", Energy Conversion and Management, Volume 49, Issue 6 (2008)

[14] Kumar Virendra, Singhal Gaurav, Subbarao P.M.V., "Study of supersonic flow in a constant rate of momentum change (CRMC) ejector with frictional effects", Applied Thermal Engineering, Volume 60, Issues 1-2 (2013)

[15] Szabolcs Varga, Pedro M.S. Lebre, Armando C. Oliveira, "CFD study of a variable area ratio ejector using R600a and R152a refrigerants", International Journal of Refrigeration, Volume 36, Issue 1 (2013)

[16] J. Fan, J. Eves, H.M. Thompson, V.V. Toropov, N. Kapur, D. Copley, A. Mincher, "Computational fluid dynamic analysis and design optimization of jet pumps", Computers & Fluids, Volume 46, Issue 1 (2011)

[17] Yinhai Zhu, Peixue Jiang, "Experimental and numerical investigation of the effect of shock wave characteristics on the ejector performance", International Journal of Refrigeration (2013)

[18] Jacek Smolka, Zbigniew Bulinski, Adam Fic, Andrzej J. Nowak, Krzysztof Banasiak, Armin Hafner, "A computational model of a transcritical R744 ejector based on a homogeneous real fluid approach", Applied Mathematical Modelling, Volume 37, Issue 3 (2013)

[19] S. He, Y. Li, R.Z. Wang, "Progress of mathematical modeling on ejectors", Renewable and Sustainable Energy Reviews, Volume 13, Issue 8, October (2009)

Appendices

Appendix I : Sample real gas modeling

All properties of gas for given local pressure and entropy are found by HEPACK software. Inlet stagnation pressure and temperature considered are 4 bar and 10K respectively.

The Mach No. is found as the ratio of fluid velocity to sonic velocity while the local cross sectional area required is found by the continuity equation for mass flow rate of 100 gps, which in turn gives the diameter of that section.

The pressure is decreased in steps for real gas modeling of nozzle until the exit pressure is reached, which is 70000 Pa in this case. Then the secondary fluid is segmented in a similar fashion until it reaches the sonic velocity to consider the ejector in double-chocking condition, which means the chocking condition applies for secondary fluid also for its maximum entrainment.

The momentum conservation and energy conservation are applied to find out the condition of fluid after mixture, which gives the velocity and enthalpy of mixed fluid. This information is again used to find the real gas properties through the HEPACK software. Finally the stagnation pressure after the shock for supersonic ejector is found to determine the maximum recoverable pressure in the diffuser.

Pressure (Pa)	Temperature (K)	Density (kg/m^3)	Enthalpy (kJ/kg-K)	Change in Enthalpy	Fluid velocity(m/s)	Sonic velocity(m/s)	Mach no.	Diameter (mm)
404000	299.615	0.648	1572496.298	2004.437	63.316	1020.202	0.062	55.710
403000	299.318	0.647	1570951.793	3548.943	84.249	1019.694	0.083	48.331
402000	299.021	0.646	1569404.989	5095.746	100.953	1019.186	0.099	44.185
401000	298.723	0.645	1567855.879	6644.857	115.281	1018.676	0.113	41.379
400000	298.425	0.644	1566304.453	8196.283	128.033	1018.165	0.126	39.294
399000	298.126	0.643	1564750.701	9750.034	139.643	1017.653	0.137	37.653
398000	297.827	0.642	1563194.615	11306.120	150.374	1017.140	0.148	36.312
397000	297.528	0.641	1561636.185	12864.550	160.403	1016.627	0.158	35.185
396000	297.228	0.640	1560075.402	14425.334	169.855	1016.112	0.167	34.218
395000	296.927	0.639	1558512.255	15988.481	178.821	1015.596	0.176	33.374
394000	296.627	0.638	1556946.736	17554.000	187.371	1015.079	0.185	32.629
393000	296.325	0.637	1555378.835	19121.901	195.560	1014.561	0.193	31.962
392000	296.023	0.636	1553808.542	20692.194	203.432	1014.042	0.201	31.362
391000	295.721	0.635	1552235.847	23839.995	211.021	1013.522	0.208	30.816
390000	295.419	0.634	1550660.740	23839.995	218.357	1013.000	0.216	30.317
389000	295.115	0.633	1549083.212	25417.523	225.466	1012.478	0.223	29.859
388000	294.812	0.632	1547503.253	26997.482	232.368	1011.955	0.230	29.435
387000	294.508	0.631	1545920.853	28579.883	239.081	1011.430	0.236	29.041
386000	294.203	0.630	1544336.001	30164.735	245.621	1010.905	0.243	28.674
385000	293.898	0.630	1542748.687	31752.049	252.000	1010.378	0.249	28.331
384000	293.592	0.629	1541158.901	33341.834	258.232	1009.851	0.256	28.008
383000	293.286	0.628	1539566.633	34934.102	264.326	1009.322	0.262	27.705
382000	292.980	0.627	1537971.873	36528.863	270.292	1008.792	0.268	27.419
381000	292.673	0.626	1536374.609	38126.126	276.138	1008.261	0.274	27.149

Pressure(Pa)	Temperature (K)	Density (kg/m^3)	Enthalpy(kJ/kg-K)	Change in Enthalpy	Fluid velocity(m/s)	Sonic velocity(m/s)	Mach no.	Diameter(mm)
355000	284.516	0.600	1493931.182	80569.554	401.421	994.050	0.404	22.999
354000	284.195	0.599	1492262.109	82238.627	405.558	993.487	0.408	22.901
353000	283.874	0.598	1490590.209	83910.527	409.660	992.923	0.413	22.805
352000	283.552	0.597	1488915.468	85585.267	413.728	992.357	0.417	22.712
351000	283.229	0.596	1487237.875	87262.860	417.763	991.790	0.421	22.621
350000	282.906	0.595	1485557.416	88943.320	421.766	991.222	0.426	22.533
349000	282.583	0.594	1483874.078	90626.658	425.739	990.653	0.430	22.447
348000	282.259	0.593	1482187.847	92312.888	429.681	990.082	0.434	22.363
347000	281.934	0.592	1480498.711	94002.025	433.594	989.510	0.438	22.281
346000	281.609	0.590	1478806.656	95694.080	437.479	988.937	0.442	22.201
345000	281.283	0.589	1477111.668	97389.068	441.337	988.362	0.447	22.123
344000	280.957	0.588	1475413.734	99087.001	445.167	987.786	0.451	22.047
343000	280.630	0.587	1473712.840	100787.895	448.972	987.209	0.455	21.972
342000	280.302	0.586	1472008.973	102491.763	452.751	986.630	0.459	21.899
341000	279.974	0.585	1470302.118	104198.618	456.505	986.051	0.463	21.828
340000	279.645	0.584	1468592.261	105908.475	460.236	985.469	0.467	21.759
339000	279.316	0.583	1466879.389	107621.347	463.943	984.887	0.471	21.691
338000	278.986	0.582	1465163.486	109337.250	467.626	984.302	0.475	21.624
337000	278.656	0.581	1463444.539	111056.197	471.288	983.717	0.479	21.559
336000	278.325	0.580	1461722.533	112778.202	474.928	983.130	0.483	21.496
335000	277.993	0.579	1459997.454	114503.281	478.546	982.542	0.487	21.433
334000	277.661	0.578	1458269.287	116231.449	482.144	981.952	0.491	21.372
333000	277.328	0.577	1456538.017	117962.719	485.722	981.361	0.495	21.313
332000	276.995	0.576	1454803.629	119697.107	489.279	980.769	0.499	21.254
331000	276.661	0.575	1453066.108	121434.628	492.818	980.175	0.503	21.197

Pressure(Pa)	Temperature (K)	Density (kg/m^3)	Enthalpy(kJ/kg-K)	Change in Enthalpy	Fluid velocity(m/s)	Sonic velocity(m/s)	Mach no.	Diameter(mm)
330000	276.327	0.574	1451325.439	123175.297	496.337	979.580	0.507	21.141
329000	275.991	0.573	1449581.606	124919.129	499.838	978.983	0.511	21.086
328000	275.656	0.572	1447834.596	126666.140	503.321	978.385	0.514	21.032
327000	275.319	0.571	1446084.390	128416.345	506.787	977.785	0.518	20.979
326000	274.982	0.570	1444330.975	130169.760	510.235	977.184	0.522	20.927
325000	274.644	0.569	1442574.335	131926.401	513.666	976.581	0.526	20.876
324000	274.306	0.568	1440814.452	133686.283	517.081	975.977	0.530	20.827
323000	273.967	0.567	1439051.313	135449.423	520.479	975.372	0.534	20.778
322000	273.628	0.566	1437284.899	137215.837	523.862	974.765	0.537	20.730
321000	273.288	0.565	1435515.196	138985.540	527.230	974.156	0.541	20.683
320000	272.947	0.563	1433742.186	140758.550	530.582	973.546	0.545	20.637
319000	272.605	0.562	1431965.853	142534.883	533.919	972.935	0.549	20.591
318000	272.263	0.561	1430186.180	144314.555	537.242	972.321	0.553	20.547
317000	271.921	0.560	1428403.152	146097.584	540.551	971.707	0.556	20.503
316000	271.577	0.559	1426616.749	147883.986	543.846	971.091	0.560	20.460
315000	271.233	0.558	1424826.957	149673.779	547.127	970.473	0.564	20.418
314000	270.888	0.557	1423033.756	151466.980	550.394	969.854	0.568	20.377
313000	270.543	0.556	1421237.130	153263.605	553.649	969.233	0.571	20.336
312000	270.197	0.555	1419437.062	155063.673	556.891	968.610	0.575	20.297
311000	269.850	0.554	1417633.534	156867.202	560.120	967.986	0.579	20.257
310000	269.503	0.553	1415826.527	158674.209	563.337	967.360	0.582	20.219
309000	269.155	0.552	1414016.024	160484.711	566.542	966.733	0.586	20.181
308000	268.806	0.551	1412202.007	162298.728	569.735	966.104	0.590	20.144
307000	268.457	0.550	1410384.458	164116.278	572.916	965.474	0.593	20.108
306000	268.107	0.549	1408563.357	165937.378	576.086	964.842	0.597	20.072

Pressure(Pa)	Temperature (K)	Density (kg/m^3)	Enthalpy(kJ/kg-K)	Change in Enthalpy	Fluid velocity(m/s)	Sonic velocity(m/s)	Mach no.	Diameter(mm)
305000	267.756	0.548	1406738.687	167762.048	579.244	964.208	0.601	20.037
304000	267.405	0.546	1404910.429	169590.306	582.392	963.572	0.604	20.002
303000	267.052	0.545	1403078.564	171422.172	585.529	962.935	0.608	19.968
302000	266.700	0.544	1401243.073	173257.663	588.656	962.296	0.612	19.935
301000	266.346	0.543	1399403.936	175096.800	591.772	961.656	0.615	19.902
300000	265.992	0.542	1397561.134	176939.602	594.877	961.013	0.619	19.870
299000	265.637	0.541	1395714.648	178786.088	597.973	960.370	0.623	19.838
298000	265.281	0.540	1393864.458	180636.278	601.060	959.724	0.626	19.807
297000	264.925	0.539	1392010.543	182490.192	604.136	959.077	0.630	19.777
296000	264.568	0.538	1390152.885	184347.851	607.203	958.427	0.634	19.747
295000	264.210	0.537	1388291.462	186209.273	610.261	957.777	0.637	19.717
294000	263.851	0.536	1386426.255	188074.481	613.310	957.124	0.641	19.688
293000	263.492	0.534	1384557.242	189943.494	616.350	956.470	0.644	19.659
292000	263.132	0.533	1382684.402	191816.333	619.381	955.813	0.648	19.631
291000	262.771	0.532	1380807.716	193693.020	622.403	955.155	0.652	19.604
290000	262.410	0.531	1378927.161	195573.575	625.418	954.496	0.655	19.577
289000	262.048	0.530	1377042.716	197458.019	628.423	953.834	0.659	19.550
288000	261.684	0.529	1375154.361	199346.375	631.421	953.171	0.662	19.524
287000	261.321	0.528	1373262.072	201238.664	634.411	952.505	0.666	19.498
286000	260.956	0.527	1371365.828	203134.908	637.393	951.838	0.670	19.473
285000	260.591	0.526	1369465.606	205035.129	640.367	951.169	0.673	19.448
284000	260.225	0.525	1367561.386	206939.350	643.334	950.498	0.677	19.423
283000	259.858	0.523	1365653.143	208847.593	646.293	949.826	0.680	19.399
282000	259.490	0.522	1363740.856	210759.880	649.246	949.151	0.684	19.376
281000	259.122	0.521	1361824.500	212676.235	652.191	948.474	0.688	19.352

Pressure(Pa)	Temperature (K)	Density (kg/m^3)	Enthalpy(kJ/kg-K)	Change in Enthalpy	Fluid velocity(m/s)	Sonic velocity(m/s)	Mach no.	Diameter(mm)
280000	258.753	0.520	1359904.054	214596.682	655.129	947.796	0.691	19.330
279000	258.383	0.519	1357979.493	216521.243	658.060	947.116	0.695	19.307
278000	258.012	0.518	1356050.794	218449.941	660.984	946.433	0.698	19.285
277000	257.640	0.517	1354117.934	220382.802	663.902	945.749	0.702	19.264
276000	257.268	0.516	1352180.887	222319.848	666.813	945.063	0.706	19.242
275000	256.895	0.515	1350239.631	224261.105	669.718	944.374	0.709	19.221
274000	256.521	0.513	1348294.139	226206.596	672.617	943.684	0.713	19.201
273000	256.146	0.512	1346344.389	228156.347	675.509	942.992	0.716	19.181
272000	255.770	0.511	1344390.353	230110.382	678.396	942.297	0.720	19.161
271000	255.394	0.510	1342432.008	232068.727	681.276	941.601	0.724	19.142
270000	255.016	0.509	1340469.328	234031.408	684.151	940.903	0.727	19.122
269000	254.638	0.508	1338502.287	235998.449	687.020	940.202	0.731	19.104
268000	254.259	0.507	1336530.859	237969.877	689.884	939.500	0.734	19.085
267000	253.879	0.506	1334555.018	239945.718	692.742	938.795	0.738	19.067
266000	253.499	0.504	1332574.738	241925.998	695.595	938.088	0.742	19.050
265000	253.117	0.503	1330589.991	243910.745	698.442	937.379	0.745	19.032
264000	252.735	0.502	1328600.751	245899.985	701.285	936.668	0.749	19.015
263000	252.351	0.501	1326606.990	247893.745	704.122	935.955	0.752	18.998
262000	251.967	0.500	1324608.682	249892.054	706.954	935.240	0.756	18.982
261000	251.582	0.499	1322605.797	251894.939	709.782	934.522	0.760	18.966
260000	251.196	0.498	1320598.309	253902.427	712.604	933.803	0.763	18.950
259000	250.809	0.496	1318586.188	255914.548	715.422	933.081	0.767	18.934
258000	250.422	0.495	1316569.406	257931.329	718.236	932.357	0.770	18.919
257000	250.033	0.494	1314547.935	259952.801	721.045	931.630	0.774	18.904
256000	249.643	0.493	1312521.744	261978.992	723.849	930.902	0.778	18.890

Pressure(Pa)	Temperature (K)	Density (kg/m^3)	Enthalpy(kJ/kg-K)	Change in Enthalpy	Fluid velocity(m/s)	Sonic velocity(m/s)	Mach no.	Diameter(mm)
255000	249.253	0.492	1310490.805	264009.931	726.650	930.171	0.781	18.875
254000	248.862	0.491	1308455.087	266045.649	729.446	929.438	0.785	18.861
253000	248.469	0.489	1306414.560	268086.175	732.238	928.702	0.788	18.848
252000	248.076	0.488	1304369.195	270131.541	735.026	927.964	0.792	18.834
251000	247.682	0.487	1302318.959	272181.776	737.810	927.224	0.796	18.821
250000	247.287	0.486	1300263.823	274236.913	740.590	926.482	0.799	18.808
249000	246.891	0.485	1298203.754	276296.981	743.367	925.737	0.803	18.796
248000	246.494	0.484	1296138.722	278362.014	746.139	924.989	0.807	18.783
247000	246.096	0.483	1294068.693	280432.042	748.909	924.240	0.810	18.771
246000	245.697	0.481	1291993.636	282507.100	751.674	923.488	0.814	18.759
245000	245.297	0.480	1289913.518	284587.218	754.437	922.733	0.818	18.748
244000	244.896	0.479	1287828.305	286672.431	757.195	921.976	0.821	18.737
243000	244.494	0.478	1285737.964	288762.771	759.951	921.217	0.825	18.726
242000	244.091	0.477	1283642.462	290858.273	762.703	920.455	0.829	18.715
241000	243.687	0.475	1281541.764	292958.971	765.453	919.690	0.832	18.705
240000	243.282	0.474	1279435.836	295064.899	768.199	918.923	0.836	18.694
239000	242.876	0.473	1277324.643	297176.093	770.942	918.153	0.840	18.684
238000	242.469	0.472	1275208.149	299292.587	773.683	917.381	0.843	18.675
237000	242.061	0.471	1273086.319	301414.417	776.421	916.606	0.847	18.665
236000	241.652	0.470	1270959.117	303541.619	779.155	915.829	0.851	18.656
235000	241.242	0.468	1268826.506	305674.230	781.888	915.049	0.854	18.647
234000	240.831	0.467	1266688.450	307812.286	784.617	914.266	0.858	18.639
233000	240.419	0.466	1264544.910	309955.825	787.345	913.481	0.862	18.630
232000	240.006	0.465	1262395.850	312104.885	790.069	912.693	0.866	18.622
231000	239.592	0.464	1260241.232	314259.504	792.792	911.902	0.869	18.614

Pressure(Pa)	Temperature (K)	Density (kg/m^3)	Enthalpy(kJ/kg-K)	Change in Enthalpy	Fluid velocity(m/s)	Sonic velocity(m/s)	Mach no.	Diameter(mm)
230000	239.176	0.462	1258081.016	316419.719	795.512	911.109	0.873	18.606
229000	238.760	0.461	1255915.164	318585.571	798.230	910.313	0.877	18.599
228000	238.342	0.460	1253743.637	320757.099	800.946	909.514	0.881	18.592
227000	237.924	0.459	1251566.394	322934.342	803.660	908.712	0.884	18.585
226000	237.504	0.457	1249383.395	325117.341	806.371	907.907	0.888	18.578
225000	237.083	0.456	1247194.599	327306.136	809.081	907.100	0.892	18.572
224000	236.661	0.455	1244999.966	329500.770	811.789	906.289	0.896	18.565
223000	236.238	0.454	1242799.453	331701.283	814.495	905.476	0.900	18.559
222000	235.814	0.453	1240593.018	333907.718	817.200	904.660	0.903	18.554
221000	235.388	0.451	1238380.618	336120.118	819.903	903.841	0.907	18.548
220000	234.962	0.450	1236162.210	338338.525	822.604	903.019	0.911	18.543
219000	234.534	0.449	1233937.751	340562.984	825.304	902.194	0.915	18.538
218000	234.105	0.448	1231707.196	342793.540	828.002	901.366	0.919	18.533
217000	233.675	0.446	1229470.500	345030.235	830.699	900.535	0.922	18.528
216000	233.244	0.445	1227227.618	347273.117	833.394	899.701	0.926	18.524
215000	232.811	0.444	1224978.504	349522.231	836.089	898.863	0.930	18.520
214000	232.378	0.443	1222723.112	351777.623	838.782	898.023	0.934	18.516
213000	231.943	0.442	1220461.395	354039.341	841.474	897.180	0.938	18.512
212000	231.507	0.440	1218193.304	356307.431	844.165	896.333	0.942	18.509
211000	231.069	0.439	1215918.793	358581.943	846.855	895.483	0.946	18.506
210000	230.631	0.438	1213637.811	360862.925	849.544	894.630	0.950	18.503
209000	230.191	0.437	1211350.310	363150.425	852.233	893.774	0.954	18.500
208000	229.750	0.435	1209056.240	365444.495	854.920	892.914	0.957	18.497
207000	229.307	0.434	1206755.550	367745.185	857.607	892.051	0.961	18.495
206000	228.863	0.433	1204448.189	370052.546	860.294	891.185	0.965	18.493

Pressure(Pa)	Temperature (K)	Density (kg/m^3)	Enthalpy(kJ/kg-K)	Change in Enthalpy	Fluid velocity(m/s)	Sonic velocity(m/s)	Mach no.	Diameter(mm)
205000	228.418	0.432	1202134.106	372366.630	862.979	890.316	0.969	18.491
204000	227.972	0.430	1199813.246	374687.489	865.664	889.443	0.973	18.489
203000	227.525	0.429	1197485.558	377015.177	868.349	888.566	0.977	18.488
202000	227.076	0.428	1195150.988	379349.748	871.034	887.686	0.981	18.487
201000	226.625	0.426	1192809.480	381691.256	873.718	886.803	0.985	18.486
200000	226.174	0.425	1190460.979	384039.756	876.401	885.916	0.989	18.485
199000	225.721	0.424	1188105.430	386395.305	879.085	885.026	0.993	18.485
198000	225.266	0.423	1185742.776	388757.959	881.769	884.132	0.997	18.484
197000	224.811	0.421	1183372.959	391127.776	884.452	883.234	1.001	18.484
196000	224.354	0.420	1180995.921	393504.814	887.136	882.333	1.005	18.485
195000	223.895	0.419	1178611.603	395889.133	889.819	881.428	1.010	18.485
194000	223.435	0.417	1176219.945	398280.791	892.503	880.520	1.014	18.486
193000	222.974	0.416	1173820.886	400679.849	895.187	879.607	1.018	18.487
192000	222.511	0.415	1171414.366	403086.370	897.871	878.691	1.022	18.488
191000	222.047	0.414	1169000.321	405500.415	900.556	877.771	1.026	18.489
190000	221.581	0.412	1166578.689	407922.047	903.241	876.848	1.030	18.491
189000	221.114	0.411	1164149.405	410351.330	905.926	875.920	1.034	18.492
188000	220.645	0.410	1161712.406	412788.330	908.612	874.988	1.038	18.494
187000	220.175	0.408	1159267.624	415233.112	911.299	874.053	1.043	18.497
186000	219.704	0.407	1156814.993	417685.742	913.987	873.113	1.047	18.499
185000	219.230	0.406	1154354.446	420146.289	916.675	872.170	1.051	18.502
184000	218.756	0.404	1151885.915	422614.821	919.364	871.222	1.055	18.505
183000	218.279	0.403	1149409.328	425091.407	922.054	870.270	1.060	18.508
182000	217.802	0.402	1146924.617	427576.118	924.744	869.314	1.064	18.511
181000	217.322	0.400	1144431.709	430069.026	927.436	868.354	1.068	18.515

Pressure(Pa)	Temperature (K)	Density (kg/m^3)	Enthalpy(kJ/kg-K)	Change in Enthalpy	Fluid velocity(m/s)	Sonic velocity(m/s)	Mach no.	Diameter(mm)
180000	216.841	0.399	1141930.533	432570.203	930.129	867.390	1.072	18.519
179000	216.358	0.398	1139421.013	435079.723	932.823	866.421	1.077	18.523
178000	215.874	0.396	1136903.076	437597.660	935.519	865.448	1.081	18.527
177000	215.388	0.395	1134376.646	440124.090	938.215	864.471	1.085	18.532
176000	214.901	0.394	1131841.646	442659.090	940.913	863.489	1.090	18.537
175000	214.412	0.392	1129297.997	445202.739	943.613	862.503	1.094	18.542
174000	213.921	0.391	1126745.621	447755.114	946.314	861.512	1.098	18.547
173000	213.428	0.390	1124184.438	450316.298	949.017	860.517	1.103	18.553
172000	212.934	0.388	1121614.365	452886.371	951.721	859.517	1.107	18.559
171000	212.438	0.387	1119035.320	455465.416	954.427	858.512	1.112	18.565
170000	211.940	0.386	1116447.219	458053.517	957.135	857.503	1.116	18.571
169000	211.441	0.384	1113849.976	460650.760	959.845	856.489	1.121	18.578
168000	210.939	0.383	1111243.504	463257.231	962.556	855.470	1.125	18.585
167000	210.436	0.382	1108627.717	465873.019	965.270	854.447	1.130	18.592
166000	209.931	0.380	1106002.523	468498.212	967.986	853.418	1.134	18.599
165000	209.425	0.379	1103367.833	471132.902	970.704	852.384	1.139	18.607
164000	208.916	0.377	1100723.554	473777.181	973.424	851.346	1.143	18.615
163000	208.406	0.376	1098069.593	476431.143	976.147	850.302	1.148	18.623
162000	207.893	0.375	1095405.853	479094.882	978.872	849.254	1.153	18.631
161000	207.379	0.373	1092732.239	481768.496	981.599	848.200	1.157	18.640
160000	206.863	0.372	1090048.653	484452.083	984.329	847.141	1.162	18.649
159000	206.345	0.371	1087354.993	487145.743	987.062	846.076	1.167	18.658
158000	205.825	0.369	1084651.159	489849.576	989.798	845.006	1.171	18.667
157000	205.303	0.368	1081937.048	492563.688	992.536	843.931	1.176	18.677
156000	204.779	0.366	1079212.554	495288.182	995.277	842.851	1.181	18.687

Pressure(Pa)	Temperature (K)	Density (kg/m^3)	Enthalpy(kJ/kg-K)	Change in Enthalpy	Fluid velocity(m/s)	Sonic velocity(m/s)	Mach no.	Diameter(mm)
155000	204.253	0.365	1076477.571	498023.165	998.021	841.764	1.186	18.697
154000	203.725	0.364	1073731.990	500768.746	1000.768	840.672	1.190	18.708
153000	203.195	0.362	1070975.701	503525.034	1003.519	839.575	1.195	18.719
152000	202.663	0.361	1068208.592	506292.143	1006.272	838.472	1.200	18.730
151000	202.128	0.359	1065430.549	509070.186	1009.029	837.363	1.205	18.741
150000	201.592	0.358	1062641.456	511859.280	1011.790	836.248	1.210	18.753
149000	201.053	0.356	1059841.194	514659.542	1014.554	835.127	1.215	18.765
148000	200.512	0.355	1057029.643	517471.093	1017.321	834.000	1.220	18.777
147000	199.969	0.354	1054206.681	520294.054	1020.092	832.867	1.225	18.790
146000	199.424	0.352	1051372.184	523128.551	1022.867	831.728	1.230	18.803
145000	198.877	0.351	1048526.025	525974.711	1025.646	830.582	1.235	18.816
144000	198.327	0.349	1045668.075	528832.661	1028.429	829.431	1.240	18.830
143000	197.775	0.348	1042798.203	531702.533	1031.215	828.273	1.245	18.844
142000	197.221	0.346	1039916.274	534584.461	1034.006	827.108	1.250	18.858
141000	196.664	0.345	1037022.154	537478.582	1036.801	825.937	1.255	18.872
140000	196.105	0.343	1034115.703	540385.033	1039.601	824.759	1.260	18.887
139000	195.544	0.342	1031196.780	543303.956	1042.405	823.574	1.266	18.902
138000	194.980	0.340	1028265.241	546235.495	1045.213	822.383	1.271	18.918
137000	194.413	0.339	1025320.940	549179.796	1048.027	821.185	1.276	18.934
136000	193.845	0.337	1022363.727	552137.009	1050.844	819.979	1.282	18.950
135000	193.273	0.336	1019393.449	555107.286	1053.667	818.767	1.287	18.966
134000	192.699	0.334	1016409.953	558090.782	1056.495	817.548	1.292	18.983
133000	192.123	0.333	1013413.080	561087.656	1059.328	816.321	1.298	19.000
132000	191.544	0.331	1010402.667	564098.068	1062.166	815.086	1.303	19.018
131000	190.962	0.330	1007378.552	567122.184	1065.009	813.845	1.309	19.036

Pressure(Pa)	Temperature (K)	Density (kg/m^3)	Enthalpy(kJ/kg-K)	Change in Enthalpy	Fluid velocity(m/s)	Sonic velocity(m/s)	Mach no.	Diameter(mm)
130000	190.378	0.328	1004340.566	570160.170	1067.858	812.595	1.314	19.054
129000	189.791	0.327	1001288.537	573212.198	1070.712	811.338	1.320	19.073
128000	189.201	0.325	998222.293	576278.443	1073.572	810.074	1.325	19.092
127000	188.608	0.324	995141.653	579359.082	1076.438	808.801	1.331	19.111
126000	188.013	0.322	992046.437	582454.298	1079.309	807.520	1.337	19.131
125000	187.415	0.321	988936.459	585564.276	1082.187	806.231	1.342	19.151
124000	186.814	0.319	985811.530	588689.206	1085.071	804.934	1.348	19.172
123000	186.210	0.318	982671.456	591829.280	1087.961	803.628	1.354	19.193
122000	185.603	0.316	979516.039	594984.696	1090.857	802.314	1.360	19.215
121000	184.993	0.315	976345.079	598155.657	1093.760	800.992	1.366	19.236
120000	184.380	0.313	973158.369	601342.367	1096.670	799.660	1.371	19.259
119000	183.764	0.311	969955.698	604545.038	1099.586	798.320	1.377	19.282
118000	183.144	0.310	966736.851	607763.884	1102.510	796.971	1.383	19.305
117000	182.522	0.308	963501.609	610999.126	1105.440	795.612	1.389	19.328
116000	181.896	0.307	960249.747	614250.989	1108.378	794.244	1.396	19.352
115000	181.268	0.305	956981.034	617519.701	1111.323	792.867	1.402	19.377
114000	180.636	0.304	953695.236	620805.499	1114.276	791.480	1.408	19.402
113000	180.000	0.302	950392.113	624108.623	1117.236	790.084	1.414	19.428
112000	179.361	0.300	947071.418	627429.318	1120.205	788.677	1.420	19.454
111000	178.719	0.299	943732.899	630767.836	1123.181	787.261	1.427	19.480
110000	178.073	0.297	940376.300	634124.436	1126.166	785.834	1.433	19.507
109000	177.424	0.295	937001.356	637499.379	1129.158	784.397	1.440	19.535
108000	176.771	0.294	933607.798	640892.938	1132.160	782.949	1.446	19.563
107000	176.115	0.292	930195.348	644305.388	1135.170	781.491	1.453	19.591
106000	175.455	0.291	926763.724	647737.012	1138.189	780.021	1.459	19.620

Pressure(Pa)	Temperature (K)	Density (kg/m^3)	Enthalpy(kJ/kg-K)	Change in Enthalpy	Fluid velocity(m/s)	Sonic velocity(m/s)	Mach no.	Diameter(mm)
105000	174.791	0.289	923312.635	651188.101	1141.217	778.541	1.466	19.650
104000	174.123	0.287	919841.784	654658.952	1144.254	777.049	1.473	19.680
103000	173.451	0.286	916350.866	658149.870	1147.301	775.546	1.479	19.711
102000	172.776	0.284	912839.568	661661.168	1150.357	774.031	1.486	19.743
101000	172.096	0.282	909307.570	665193.166	1153.424	772.504	1.493	19.775
100000	171.413	0.281	905754.543	668746.193	1156.500	770.965	1.500	19.808
99000	170.725	0.279	902180.149	672320.587	1159.587	769.413	1.507	19.841
98000	170.033	0.277	898584.042	675916.694	1162.684	767.849	1.514	19.875
97000	169.337	0.276	894965.866	679534.870	1165.791	766.273	1.521	19.909
96000	168.637	0.274	891325.257	683175.479	1168.910	764.683	1.529	19.945
95000	167.932	0.272	887661.838	686838.897	1172.040	763.080	1.536	19.981
94000	167.223	0.270	883975.226	690525.510	1175.181	761.463	1.543	20.017
93000	166.509	0.269	880265.023	694235.712	1178.334	759.833	1.551	20.055
92000	165.791	0.267	876530.823	697969.913	1181.499	758.188	1.558	20.093
91000	165.068	0.265	872772.207	701728.529	1184.676	756.530	1.566	20.132
90000	164.340	0.263	868988.743	705511.992	1187.865	754.856	1.574	20.171
89000	163.607	0.262	865179.990	709320.746	1191.067	753.168	1.581	20.212
88000	162.869	0.260	861345.490	713155.245	1194.282	751.464	1.589	20.253
87000	162.126	0.258	857484.775	717015.961	1197.511	749.745	1.597	20.295
86000	161.378	0.256	853597.359	720903.376	1200.753	748.011	1.605	20.338
85000	160.625	0.255	849682.746	724817.990	1204.008	746.259	1.613	20.382
84000	159.867	0.253	845740.420	728760.315	1207.278	744.492	1.622	20.427
83000	159.103	0.251	841769.853	732730.883	1210.563	742.707	1.630	20.472
82000	158.333	0.249	837770.497	736730.239	1213.862	740.906	1.638	20.519
81000	157.558	0.247	833741.789	740758.946	1217.176	739.086	1.647	20.567

Pressure(Pa)	Temperature (K)	Density (kg/m^3)	Enthalpy(kJ/kg-K)	Change in Enthalpy	Fluid velocity(m/s)	Sonic velocity(m/s)	Mach no.	Diameter(mm)
80000	156.777	0.245	829683.148	744817.588	1220.506	737.249	1.655	20.615
79000	155.990	0.244	825593.971	748906.764	1223.852	735.393	1.664	20.665
78000	155.198	0.242	821473.639	753027.097	1227.214	733.518	1.673	20.715
77000	154.399	0.240	817321.510	757179.226	1230.593	731.624	1.682	20.767
76000	153.594	0.238	813136.920	761363.816	1233.989	729.711	1.691	20.820
75000	152.782	0.236	808919.183	765581.553	1237.402	727.777	1.700	20.874
74000	151.964	0.234	804667.590	769833.146	1240.833	725.822	1.710	20.929
73000	151.139	0.232	800381.405	774119.331	1244.282	723.846	1.719	20.985
72000	150.308	0.230	796059.867	778440.869	1247.751	721.848	1.729	21.043
71000	149.469	0.229	791702.187	782798.549	1251.238	719.828	1.738	21.102
70000	148.624	0.227	787307.547	787193.189	1254.746	717.786	1.748	21.162
69000	147.771	0.225	782875.099	791625.637	1258.273	715.719	1.758	21.224
68000	146.910	0.223	778403.961	796096.774	1261.822	713.629	1.768	21.287
67000	146.042	0.221	773893.221	800607.515	1265.391	711.514	1.778	21.352
66000	145.167	0.219	769341.927	805158.808	1268.983	709.374	1.789	21.418
65000	144.283	0.217	764749.092	809751.643	1272.597	707.208	1.799	21.486
64000	143.391	0.215	760113.689	814387.046	1276.234	705.014	1.810	21.555
63000	142.491	0.213	755434.649	819066.087	1279.895	702.794	1.821	21.626
62000	141.582	0.211	750710.857	823789.879	1283.581	700.545	1.832	21.699
61000	140.664	0.209	745941.153	828559.583	1287.291	698.266	1.844	21.773
60000	139.737	0.207	741124.327	833376.408	1291.028	695.958	1.855	21.850
59000	138.801	0.205	736259.117	838241.619	1294.791	693.619	1.867	21.928
58000	137.855	0.202	731344.202	843156.533	1298.581	691.248	1.879	22.009
57000	136.899	0.200	726378.205	848122.530	1302.400	688.844	1.891	22.091
56000	135.934	0.198	721359.685	853141.051	1306.247	686.406	1.903	22.176

Pressure(Pa)	Temperature (K)	Density (kg/m^3)	Enthalpy(kJ/kg-K)	Change in Enthalpy	Fluid velocity(m/s)	Sonic velocity(m/s)	Mach no.	Diameter(mm)
55000	134.957	0.196	716287.132	858213.604	1310.125	683.933	1.916	22.263
54000	133.971	0.194	711158.965	863341.771	1314.033	681.424	1.928	22.353
53000	132.973	0.192	705973.528	868527.208	1317.974	678.877	1.941	22.445
52000	131.963	0.190	700729.082	873771.654	1321.947	676.292	1.955	22.539
51000	130.942	0.187	695423.800	879076.936	1325.954	673.667	1.968	22.637
50000	129.909	0.185	690055.762	884444.974	1329.996	671.000	1.982	22.737
49000	128.864	0.183	684622.948	889877.788	1334.075	668.290	1.996	22.840
48000	127.806	0.181	679123.230	895377.506	1338.191	665.536	2.011	22.946
47000	126.734	0.178	673554.362	900946.374	1342.346	662.736	2.025	23.056
46000	125.648	0.176	667913.976	906586.760	1346.541	659.887	2.041	23.169
45000	124.549	0.174	662199.568	912301.168	1350.778	656.989	2.056	23.285
44000	123.434	0.172	656408.486	918092.249	1355.059	654.039	2.072	23.406
43000	122.304	0.169	650537.925	923962.810	1359.384	651.034	2.088	23.530
42000	121.159	0.167	644584.905	929915.830	1363.756	647.974	2.105	23.659
41000	119.996	0.164	638546.262	935954.473	1368.177	644.854	2.122	23.792
40000	118.817	0.162	632418.630	942082.106	1372.649	641.673	2.139	23.930
39000	117.620	0.160	626198.420	948302.315	1377.173	638.428	2.157	24.072
38000	116.404	0.157	619881.806	954618.930	1381.752	635.116	2.176	24.220

Furthermore, the secondary stream has discretised from pressure of 80000 Pa until it reaches the sonic velocity, as ejector has been designed for double chocking condition.

Pressure(Pa)	Temperature (K)	Density (kg/m^3)	Enthalpy(kJ/kg-K)	Change in Enthalpy	Fluid velocity(m/s)	Sonic velocity(m/s)	Mach no.	Cross sectional area(m^2)
79000.000	198.996	0.191	1048930.822	5215.652	102.134	830.462	0.123	1281.503
78000.000	197.985	0.190	1043675.426	10471.048	144.714	828.346	0.175	911.374
77000.000	196.966	0.188	1038379.465	15767.008	177.578	826.208	0.215	748.476
76000.000	195.939	0.187	1033042.096	21104.378	205.448	824.048	0.249	652.035
75000.000	194.903	0.185	1027662.441	26484.033	230.148	821.865	0.280	586.698
74000.000	193.860	0.184	1022239.596	31906.878	252.614	819.658	0.308	538.841
73000.000	192.808	0.182	1016772.622	37373.852	273.400	817.428	0.334	501.953
72000.000	191.747	0.181	1011260.548	42885.925	292.868	815.173	0.359	472.478
71000.000	190.677	0.179	1005702.369	48444.105	311.269	812.893	0.383	448.292
70000.000	189.598	0.178	1000097.040	54049.433	328.784	810.587	0.406	428.037
69000.000	188.510	0.176	994443.480	59702.994	345.552	808.255	0.428	410.796
68000.000	187.413	0.175	988740.564	65405.910	361.679	805.896	0.449	395.930
67000.000	186.306	0.173	982987.127	71159.347	377.252	803.508	0.470	382.974
66000.000	185.188	0.171	977181.955	76964.518	392.338	801.092	0.490	371.584
65000.000	184.061	0.170	971323.791	82822.683	406.996	798.647	0.510	361.496
64000.000	182.923	0.168	965411.322	88735.152	421.272	796.171	0.529	352.508
63000.000	181.774	0.167	959443.185	94703.289	435.209	793.664	0.548	344.458
62000.000	180.615	0.165	953417.959	100728.515	448.840	791.125	0.567	337.217
61000.000	179.444	0.164	947334.163	106812.310	462.195	788.554	0.586	330.682
60000.000	178.261	0.162	941190.255	112956.219	475.302	785.948	0.605	324.767
59000.000	177.067	0.160	934984.622	119161.852	488.184	783.307	0.623	319.401

Pressure(Pa)	Temperature (K)	Density (kg/m^3)	Enthalpy(kJ/kg-K)	Change in Enthalpy	Fluid velocity(m/s)	Sonic velocity(m/s)	Mach no.	Cross sectional area(m^2)
58000.000	175.861	0.159	928715.582	125430.892	500.861	780.631	0.642	314.525
57000.000	174.641	0.157	922381.376	131765.098	513.352	777.917	0.660	310.089
56000.000	173.409	0.155	915980.166	138166.308	525.673	775.165	0.678	306.052
55000.000	172.164	0.154	909510.027	144636.447	537.841	772.373	0.696	302.379
54000.000	170.905	0.152	902968.942	151177.532	549.868	769.541	0.715	299.038
53000.000	169.632	0.150	896354.797	157791.677	561.768	766.666	0.733	296.003
52000.000	168.345	0.149	889665.374	164481.100	573.552	763.747	0.751	293.253
51000.000	167.042	0.147	882898.344	171248.130	585.232	760.784	0.769	290.767
50000.000	165.724	0.145	876051.256	178095.218	596.817	757.773	0.788	288.529
49000.000	164.391	0.143	869121.533	185024.941	608.317	754.714	0.806	286.525
48000.000	163.040	0.142	862106.460	192040.014	619.742	751.605	0.825	284.743
47000.000	161.673	0.140	855003.174	199143.300	631.100	748.444	0.843	283.172
46000.000	160.288	0.138	847808.652	206337.822	642.398	745.228	0.862	281.803
45000.000	158.885	0.136	840519.699	213626.775	653.646	741.956	0.881	280.629
44000.000	157.464	0.134	833132.936	221013.538	664.851	738.625	0.900	279.643
43000.000	156.022	0.133	825644.779	228501.695	676.020	735.233	0.919	278.842
42000.000	154.561	0.131	818051.430	236095.044	687.161	731.778	0.939	278.220
41000.000	153.078	0.129	810348.852	243797.622	698.280	728.256	0.959	277.775
40000.000	151.574	0.127	802532.749	251613.725	709.385	724.665	0.979	277.507
39000.000	150.047	0.125	794598.546	259547.928	720.483	721.002	0.999	277.413
38000.000	148.496	0.123	786541.360	267605.114	731.581	717.262	1.020	277.495